Summer 8-2014

Single Tube, Multiple Enzyme Reaction for Detection of UV and Oxidative Damage in Forensic Physiological Stains

Nicholas J. Eurek
University of Nebraska-Lincoln, neurek88@gmail.com

SINGLE TUBE, MULTIPLE ENZYME REACTION FOR DETECTION OF UV AND OXIDATIVE DAMAGE IN FORENSIC PHYSIOLOGICAL STAINS

By

Nicholas J. Eurek

A THESIS

Presented to the Faculty of
The Graduate College at the University of Nebraska
In Partial Fulfillment of Requirements
For the Degree of Master of Science

Major: Biochemistry

Under the Supervision of Professor Ashley M. Hall

Lincoln, Nebraska

August, 2014

SINGLE TUBE, MULTIPLE ENZYME REACTION FOR DETECTION OF UV AND OXIDATIVE DAMAGE IN FORENSIC PHYSIOLOGICAL STAINS

Nicholas Eurek, M.S.

University of Nebraska, 2014

Advisor: Ashley Hall

For decades, the use of DNA as a biological tool has revolutionized forensic investigations. The primary use of this genetic evidence is for identification of a victim or suspect through short tandem repeat (STR) profiling. However, the usefulness of this evidence can be compromised through inhibition of PCR, damage to the DNA, or low copy number. Here, we investigate damage induced to DNA by environmental factors.

UV light is known to damage DNA by the formation of cyclobutane pyrimidine dimers, 6-4 photoproducts, and strand breaks. These lesions can stall polymerase action or misincorporate bases during extension. Oxidative damage is also common to environmentally exposed samples and can occur by microbial digestion or radiation. The primary lesion associated with oxidative damage is the formation of 8-oxoguanine, which can result in base modification.

A novel assay involving a glycosylase and S1 enzymatic digestion to convert damage lesions to double strand breaks was developed to investigate damage associated with environmental exposure. Both reactions have enzyme activity in the same buffer, thus samples can be processed in the same tube to minimize the loss of DNA by transfer. Because double strand instead of single strand breaks are evaluated, samples can be

evaluated on a native agarose gel which is more sensitive than damage detection techniques such as an alkaline agarose gel.

Following optimization of the glycosylase plus S1 reaction, this assay was used as a tool to asses UV and oxidative damage in bloodstains exposed to the environment. The physiological stains were left uncovered to the environment for time points ranging from 1 day to 6 months. A sharp decrease in yield was observed for DNA exposed to the environment for more than 5 days. Samples exposed to environmental insults for 3 and 5 days exhibited both UV and oxidative damage as well as strand breaks. Oxidative damage was determined to constitute a higher number of damage lesions than UV damage. STR profiling revealed this damage did not result in a loss of genetic profile through 5 days of exposure.

ACKNOWLEDGEMENTS

I would like to first thank my advisor, Dr. Ashley Hall, who guided me through the completion of this work. I am extremely appreciative for the opportunity to join her lab and further my education. Her research experience and guidance were invaluable to me throughout my thesis. Dr. Hall has many creative and inspiring research strategies that are applicable to the field of forensic science and I am grateful that I was able to be a small part of these research endeavors. I also appreciate her patience and understanding while serving as her research assistant. Dr. Hall has been a tough but fair mentor, who pushed me to my intellectual limits and greatly influenced my development as a scientist.

My two other committee members were also large contributors to my success. Drs. Melanie Simpson and Nick Miller constantly made me question and evaluate my research which lead me to develop a better understanding of its purpose and whether or not my objectives were being met. Their guidance was helpful in troubleshooting various problems that arose throughout my graduate career. I would also like to acknowledge those who donated body fluids needed for research during the course of this study as my experiments would not be possible without these donations.

Finally, I would like to thank my friends and family, who supported me in this endeavor and understood that my free time for seeing them was at a premium. Specifically, I am thankful for my parents, Mark and Patty, who instilled a hardworking mindset in me from an early age. They encourage me to be a better person and support me when facing life's obstacles. They value education and imparted those ideals onto me as well as their other children. Finally, I would like to thank my girlfriend, Kimmie Fox,

who never complained when I would come home stressed, stayed by my side all night while I was working on papers, and always made sure I was well-fed. I truly could not have made it this far without her support.

TABLE OF CONTENTS

LIST OF FIGURES

LIST OF TABLES

ACRONYMS

6-4 PPs- 6–4 photoproducts

8-oxoguanine- 8-oxo-7,8-dihydroguanine

AP site- apurinic/apyrimidinic site

BER- base excision repair

bp- base pair

BSA- bovine serum albumin

CE- capillary electrophoresis

Cq- quantification cycle

CODIS- combined DNA index system

CPD- cyclobutane pyrimidine dimer

DNA- deoxyribonucleic acid

DSB- double strand break

FPG- formamidopyrimidine dimer glycosylase

LCN- low copy number

Lord-Q- long-run rtPCR technique for DNA damage quantification

NAMW- number average molecular weight.

NEB- New England Biolabs

PCR- polymerase chain reaction

qPCR- quantitative polymerase chain reaction

RFLP- restriction fragment length polymorphism

RFU- relative fluorescent unit

Thymine glycol- 5,6-dihydroxy-5,6-dihydrothymidine

SSB- single strand break

STR- short tandem repeat

T4PDG- T4 pyrimidine dimer glycosylase

UV- ultraviolet

CHAPTER 1

LITERATURE REVIEW

Introduction

Genotyping by short tandem repeat (STR) profiling has become a staple of the field of forensic science and a means by which valuable individual trace evidence is generated for investigators. STR profiles have a high power of discrimination which ultimately can aid in criminal investigations to associate evidence with an individual. Because DNA is a highly reactive chemical structure, it is subject to insults that could take away this power of discrimination by complicating STR analysis. Specifically, damage due to ultraviolet (UV) radiation and oxidative damage has been known to affect the primary structure of DNA, which can affect the utilization of this type of evidence.

Limited research has been conducted in regards to what type of damage is typically seen in the DNA collected from bodily fluids found at crime scenes. This information could be valuable in determining DNA repair strategies to recover genotypic profiles and restore the power of discrimination associated with the collected evidence.

STR Profiling

STR profiling has shown to be of immense importance in the analysis of evidence. Sources of DNA can be found at nearly every crime scene and thus a genetic profile is a key piece of evidence in criminal investigations. Due to the highly polymorphic nature of the alleles used in STR profiling, there is a high level of variance between the profiles of different individuals. Thirteen loci are required to be correctly typed for the profile to be submitted to the combined DNA index system (CODIS) (1). The probability that a certain genotype is present in a given population is determined by multiplying the frequencies of each allele. These allelic frequencies are calculated based

on equations derived from the Hardy-Weinberg equilibrium (2). The Hardy-Weinberg equilibrium is a set of assumptions that can be used to calculate the genotype frequency from the frequencies of the different alleles. When 13 or more loci are correctly called, the probability of another person in the population having that same genotypic profile can be more than 1 in 1 trillion (3).

An STR profile is generated by amplification of variable regions of DNA using a multiplex of different primers. These primers are tagged with different fluorescent dyes and anneal to loci typically containing repeat elements at a length between 2-5 bp. These STRs are selected for inclusion within this multiplex because they are highly polymorphic, which allows profiles to be distinguishable. PCR produces amplicons that contain sequences of DNA that correlate to the alleles of the loci.

The most common method of detecting the amplicons produced by the multiplex reaction is to use capillary electrophoresis (CE). This technique is high throughput and highly sensitive (4). Briefly, amplicons, generated by PCR, are injected into the capillary containing polymer. The polymer creates a matrix through which the amplicons are separated by the application of an electrical current; similar to how a matrix created by agarose separates DNA based on its molecular weight when gel electrophoresis is performed. Once the amplicons reach the laser detection window, the fluorescent tags contained on the primers are excited and emit fluorescence measured in relative fluorescent units (RFU). Because the primers are labeled with different dye sets, multiple loci, correlating to the same size range, can be detected in a single run based on the color of fluorescence emitted. A lane standard, labeled with a dye separate from the STR loci, is always run congruently with each injection as it will serve as both a positive control for

CE and as a marker for the base pair size of the amplicons. Thus, each fluorescent peak represents an allele of the genotype which can be identified based on the dye used to label its primers and the length of the amplicon, based on the migration through the capillary. For STR loci, alleles usually vary by different multiples of the repeat unit. Population statistics is then used as a tool to analyze the data and describe the probability that same genotype exists in a given population.

Evaluating Low Copy Number Samples

Low quantity DNA has been known to cause issues in STR profiling. Samples containing a quantity of DNA below 100 pg are termed low copy number (LCN) and typically exhibit a variety of stochastic characteristics (5). These effects can compromise the ability to genotype the DNA and determine the source of the genetic material (6). The characteristics of stochastic effects include allelic drop in and drop out, increased stutter peaks, and heterozygous peak imbalance (7). Though many techniques have been researched, none have been able to completely eliminate the existence of these negative effects in LCN samples.

Drop in and drop out alleles are common stochastic effects seen in LCN samples. Allelic drop out is due to the preferential amplification of one allele at one or more heterozygous loci (8). This effect is often seen first in loci with larger amplicons in degraded DNA. Allelic drop in, on the other hand, results from the noise associated with LCN samples. Artifacts and background noise can lead to extra peaks in the generated electropherogram that complicate the results thus making genotyping difficult (9).

Multiple peaks in the genotype can also result from unexpected DNA in the

sample either due to multiple donors related to the genetic sample or outside contamination. A mixed donor sample contains more than one source of DNA. The individual profiles of each donor must be known to determine which alleles are associated with each individual. Collection of the evidence could also lead to extraneous DNA in the sample. This contamination of a second source of DNA from the investigators can occur directly at the crime scene or after the sample has been collected (5). Many labs will generate genetic profiles of everyone on staff before the collection of evidence in an attempt to reduce the effect of this contamination.

An increase in stutter peaks is another stochastic effect associated with low copy number or degraded samples. Stutter peaks result from the slipped strand mispairing during the extension step of PCR (10). The slippage typically takes place when the polymerase pauses allowing the duplex DNA to "breath" and a strand to loop out of the rest of the sequence upon annealing back to the template. If the nascent strand becomes mis-aligned, then additional DNA bases will be inserted after polymerase extension. If the mis-alignment occurs in the template sequence, a deletion would result with the looped out region being left out. This process has a greater likelihood of forming with repetitive elements as the strand has a tendency to anneal to a different repetitive sequence resulting formation of a looped out sequence. If these products are generated early in the cycle, they will continue to be amplified during the PCR process. The percentage of stutter peak in relation to the parent peak is variable, making calling the correct alleles in the genotype difficult (6). Thus, only RFU peaks at or below the threshold of 15 to 20% of the parent peak are termed stutter peaks that can be removed from analysis.

Finally, an increase in heterozygote allele imbalance within a locus can occur in LCN samples (9). The same stochastic sampling and amplification effects that cause drop-out alleles also cause the large difference in relative fluorescence units seen between alleles, and can create difficulties when trying to characterize heterozygosity at a certain locus. It is sometimes difficult to determine whether a second peak in the data is a result of heterozygous imbalance or stutter.

Recently, research has been conducted to obtain STR profiles from small amounts of starting genetic material. LCN DNA is associated with cases in which minimal amounts of genetic material can be found including, but not limited to, touch samples, bedding, or sweat (11). A variety of tactics have been employed to try to increase the quality of the profile obtained from these samples including: increased cycle number, reduced PCR reagent volume, and post-PCR product cleanup (9).

Increasing the number of cycles during PCR amplification is the most common method of analyzing trace amounts of DNA in order to generate a reliable profile. The standard number of cycles is 28, which can be increased to 34 with minimal effort. In theory, this small increase in cycle number enhances the PCR product by over 3 billion copies (5). However, this product increase also includes amplification of artifacts related to the LCN samples. Increasing cycle number increases stochastic effects such as heterozygous imbalance, stutter products, drop-in and profile imbalance (8).

A reduced PCR reagent volume is another useful method to obtain a genetic profile from LCN samples. Lowering the PCR reagent volume will increase molecular crowding of the reagents, thus heightening the chance of molecules colliding into one

another to form a reaction (12). This means that smaller amounts of starting DNA can produce results similar to larger-scale reactions that contain a higher quantity of DNA and a larger reagent volume (13). For example, 0.5 ng of DNA in a 10 µL PCR reaction volume should produce an identical profile to 2 ng of the same DNA in a 40 µL reaction. Reagents including polyethylene glycol, dextran, and bovine serum albumin (BSA) could also be added to the reaction to increase molecular crowding *in vitro*.

Post-PCR purification is a technique that is useful in producing the highest resolution profiles during CE analysis. This purification removes ions that compete with DNA during electrokinetic injection. The injection typically lasts 5 sec, so to obtain the highest electropheric peak, the sample should be as pure as possible. Studies have shown that the peak heights, measured in RFU, can be increased by up to four times by purification using Minelute columns (Qiagen, Valencia, CA) (14). By removing unwanted ions in the sample, a full profile could be obtained from as little as 20 pg of DNA, equivalent to the human genomic DNA contained in four cells (14). Though peak heights can be increased by this method, there are a number of stochastic effects also observed which include stutter peaks and heterozygous imbalance.

UV Damage

Ultraviolet light can be classified into three different ranges including UVA (320-400 nm), UVB (280-320nm), or UVC (100-280nm). The most lethal of these forms is UVC; however, this wavelength is absorbed by the atmosphere before reaching the Earth's surface and does not pose a threat in regards to cases of damaging DNA. Thus, the portion of the UV light spectrum that would affect forensic type samples includes UVA and UVB light. Of the total energy of this spectrum, UVA accounts for 90-99% and

UVB 1-10% of the rays that reach the Earth's surface (15).

Though UV formation has not be extensively studied in a forensic context, it has been studied in genetic disease and cancer research. Thus, many of the molecular mechanisms have already been determined in model systems. This includes mechanisms of the formation as well as the repair of this damage.

UV light exposure has the potential to cause a variety of lesions in DNA. The most prevalent of these in the physiological B conformation is the formation of cyclobutane pyrimidine dimers (CPDs) accounting for 75% of the UV damage; however, the formation of this lesion is dependent on the sequence content (16, 17). Recently, it was shown that CPD hotspots typically form around repeat elements, such as *Alu* (18). These sequences have a unique chromatin environment that allows for rearrangement during repair. Cyclobutane pyrimidine dimers are predominantly located between adjacent thymine (TT) base pairs, but formation also occurs between TC, CT, or CC adjacent bases (19). UV light causes a saturation of the 5,6 double bond between pyrimidine bases which leads to covalent linkages and the formation a cyclobutane ring (20). The predominant conformation of this ring structure is cis-syn with the minor form being trans-syn isomers which are formed at a rate of 2% of that of the cis-syn isomer (21). This ring formation could disrupt base stacking and complementary pairing in the native B-DNA conformation leading to polymerase stalling or misincorporation of bases during PCR extension (19).

6–4 photoproducts (6-4 PPs) are another alteration to the structure of DNA caused by UV radiation. This alteration occurs, as indicated by its name, when a sigma bond is

formed between the C_6 position of one pyrimidine and the C_4 position of an adjacent pyrimidine. An intermediate is needed for the reaction to proceed. Transfer of the C_4 hydroxyl or amino group on one pyrimidine to the C_5 bond of other base forms an oxetane intermediate (22). Both dimers could lead to changes in the length of both the major and minor grooves of DNA due to alterations of the helix structure (23). Such alterations will interfere with the replication and transcription machinery by weakening the affinity of the polymerase for the local and global structure of the DNA substrate (19).

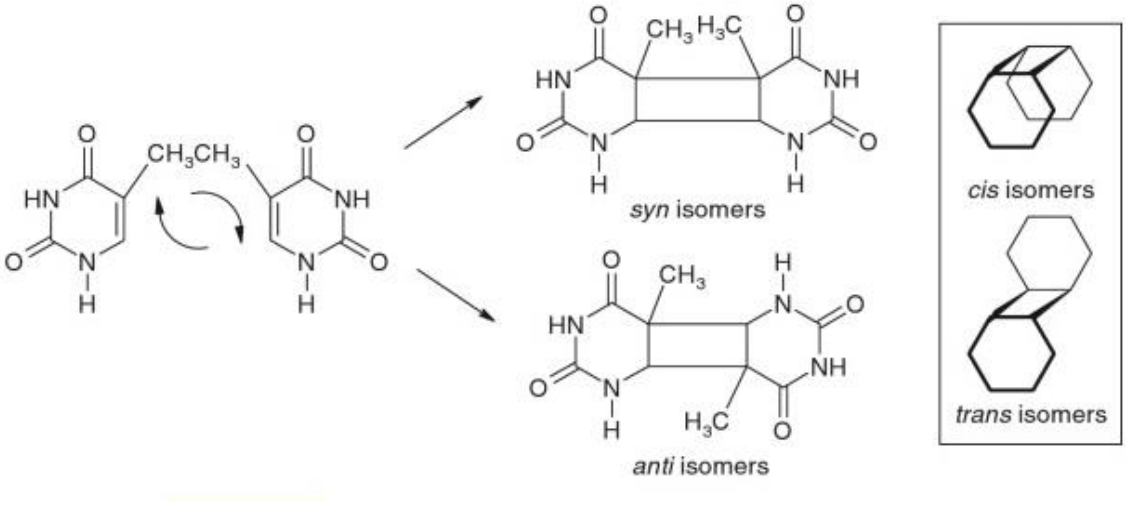

Figure 1-Thymine Dimer Formation by UV Light. Thymine dimer formation by UV light proceeds in either the cis or trans conformation. Figure from Douki (24).

Oxidative Damage

Another important and common type of damage in forensic DNA samples is oxidative damage. Oxidative damage is formed due to exposure to OH radicals, one-electron oxidants and singlet oxygen (25). This can be due to either ionizing radiation or metabolic processes (26). Though a multitude of different lesions can be induced by

oxidative insults, the primary form of damage is the alteration of the guanine base to 8-oxo-7,8-dihydroguanine, commonly referred to as 8-oxoguanine. This residue is typically used as a biomarker of oxidative stress because it is formed by any of the above mentioned sources (27). 8-oxoguanine is formed by hydroxyl attack of guanine leading to the generation of 8-hydroxy-7,8-dihydro-7-yl, a radical intermediate (27). Oxidation of this intermediate leads to the formation of 8-oxo-guanine, while reduction produces formamidopyrimidine (FAPY).

In terms of the effect oxidative damage has on genotyping samples, 8-oxo-guanine can result in a miscoding of bases during PCR amplification as the guanine base would pair with an adenine instead of cytosine (28). If this miscoding were to occur in the primer region, the primers may not bind due to the primer sequence no longer possessing complementarity to the target sequence. This would prevent the polymerase from initiating replication to the target DNA with base modifications to the 5' end of the primer region would have a more pronounced effect (29). Oxidation could also lead to the formation of hydrations that are not recognized by *Taq* polymerase and inhibit PCR amplification (30). The alteration of bases leading to mutagenic lesions could interfere with SNP typing, which assays for single nucleotide mutations as a means of distinguishing an individual. This technique requires more SNP sites to obtain the same power of discrimination observed with STR profiling, which is a major reason why STR profiling is often favored.

In addition to the alteration of guanine bases, thymine bases are another base subject to oxidative stress. Six different oxidative products can be formed by the reaction of a hydroxyl with thymine consisting of four cis and trans diastereomers of 5,6-

dihydroxy-5,6-dihydrothymidine (thymine glycol) and the methyl oxidation products 5-(hydroxymethyl)-2'-deoxyuridine and 5-formyl-2'-deoxyuridine (27). Thymine glycol is the primary lesion to thymine bases. Typically, the initial step of this alteration involves an addition of the hydroxyl to C5 bond, but addition of the hydroxyl can also occur, to a lesser extent, at the C6 bond (31). Thymine glycol modification can block polymerase replication and in fewer instances cause base mutations to the DNA (32).

Other modification by oxidative damage include strand breaks, modifications to the sugar residue, abasic sites, and protein cross-links. Hydroxyl radicals have been known to mediate strand breaks at the C3, C4, and C5 of the 2-deoxyribose sugar moiety (33). Modifications of sugar can result in tandem and interstrand 2-deoxyribose base adducts (34). Free radicals can interact with protein in the chromatin to form covalent DNA-protein-cross links. Thus, oxidative damage has the ability to affect the structure of DNA through number way, many of which could affect STR profiling or produce base mutations.

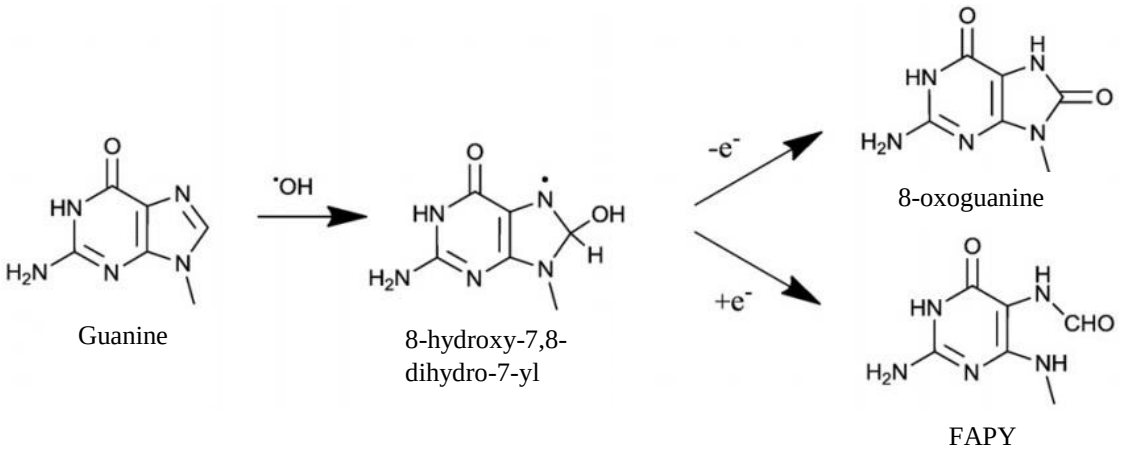

Figure 2- Mechanism of 8-oxo-guanine Formation by Oxidation. Hydroxyl radical attack to guanine results in the formation of the 8-hydroxy-7,8-dihydro-7-yl radical intermediate. Further oxidation (denoted by $-e^-$) results in generation of 8-oxo-guanine and reduction (denoted by $+e^-$) forms FAPY. Adapted from Cadet et al. (27).

Hydrolysis

Hydrolysis can release nucleic acids by hydrolytic cleavage of the glycosyl bonds of DNA in aqueous solution. This was experimentally determined initially by using ^{14}C-labeled purine and pyrimidines to measure the rate at which bases were released as a function of temperature, pH, and ionic strength (35, 36). *In vivo*, the strand breaks due to hydrolysis of cells is countered by repair strategies of the organism initiated by AP endonucleases (37). With regard to forensic samples, most repair enzymes would no longer be active as the cells are no longer physiologically active and are categorized as in the dry state. Hydrolysis as a result of the loss of bases has been observed in ancient DNA. Depurination is the most important route of decay for ancient DNA as pyrimidines are released at a mere 5% of this rate (37). A loss of base is often followed by β elimination reaction which break the sugar-phosphate backbone leading to strand scission. Besides base loss, hydrolysis can also modify bases. Hydrolytic deamination

results in a loss of the amine group for adenine, cytosine, 5-methylcytosine and guanine with cytosine being the residue most prone to this reaction (37). Loss of an amine group often results in misincorporation of bases during PCR as this modification disrupts base pairing.

Analysis of hydrolysis of DNA in the forensically relevant dry state found that the mechanism of damage is the same for hydrated and dry state samples; however, hydrolysis rates were much faster in the hydrated samples as compared to the dry state (38). Using HPLC analysis, depurination was found to be more significant than deamination reactions in the dried blood stains. A duplex configuration of DNA offers some protection from hydrolysis for both states of DNA as there is less opportunity for water molecules to interact with the pyrimidines and purines (37, 39). Thus, for both ancient DNA and contemporary forensic stains depurination is the most significant damaging factor by the hydrolysis mechanism.

Characterization of Damaged Samples

Few researchers have undertaken the task of understanding what DNA damage typically comprises an environmentally damaged forensic (body fluid) stain. This information could be useful for development of repair/recovery strategies and also give clues about the length of time DNA could survive in a given environmental scenario. Unfortunately, environmental damage studies can be difficult to control when looking at samples exposed to the elements. For this reason, some researchers have chosen to look at how each component affect STR profiling.

Hall and Ballantyne worked on characterizing the UV component of

environmental damage. They found that strand breaks were a more common source of damage than CPDs when exposed to UVC light and proposed that dehydrated DNA is less likely to form thymine dimers than hydrated DNA due to changes in conformation (40). Later, they analyzed the UVB and UVA component of UV damage and found that UVA had no effect on the ability to generate an STR profile, but with sufficient UVB damage, allelic dropout was observed (41). They theorized that oxidative damage could also play a role in this dropout, but more sensitive assays for detection would need to be administered in order to determine this. Of the sources of DNA tested, bloodstains were the first to exhibit allele dropout followed by cell-free solubilized DNA and allele dropout was not present in cell-free dehydrated DNA (41). Though the cellular milieu affords the DNA some protection from damage, other cell components including photosensitizers and the iron in heme could have promoted the damage that resulted in profile loss for the bloodstains.

Looking at the overall damaged induced, McNally et al. analyzed environmentally damaged samples of forensic cases in New York City (42). Their research examined the effect that exposure to environmental conditions has on restriction fragment length polymorphism (RFLP) analysis. The authors first examined the DNA on a native agarose gel to determine if it was of sufficient quality to be evaluated using RFLP. Native gel electrophoresis showed that over half of the 100 samples analyzed contained degraded DNA demonstrating how common damage is to case like samples. RFLP analysis was performed only on the samples that were not degraded or only partially degraded and results were obtained for some samples.

Ballantyne et al also examined forensic stains that were subject to environmental

damage in Orlando, Florida. The objective of this experiment was to investigate methods of recovering STR profiles from damages or degraded samples (43). Bloodstains were left outside, uncovered for time points extending from 0 until 9 weeks. Partial allelic dropout was observed after 3 days and a complete loss of the profile after 7 days (43). Researchers theorized that the rapid amount of damage formed was due to strand breaks induced by microorganisms. Onori et al. exposed bloodstains and tissues to various environmental locale such as open air, buried, and wet scenarios (44). Bloodstains in a wet environment were the first to exhibit dropout of the allelic profile and decreased quantification; however, allelic dropout was seen in both dry and wet bloodstains as well as the tissue samples within a week of deposition. Thus, all samples types were subject to allelic dropout but the most rapid loss of profiling data occurred in wet samples. This demonstrates that more damage and loss of genotyping ability could be due to hydrolysis, adoption of the hydrated B-form DNA confirmation or damaging agents having better access to DNA due to the solution chemistry versus the A-form associated with dehydrated DNA.

Sources of Environmental Damage

Environmental insults to DNA can originate from a variety of sources. Large contributors to this damage include microorganisms and atmospheric conditions; both of which will vary depending on the geographic location of the sample and local environment. It is believed that environmental damage is responsible for the majority of damage lesions to DNA recovered from physiological stains at a crime scene although it has not been demonstrated conclusively which type of environmental damage is the major contributor. This damage can result in a loss of signal in STR profiling making

genotyping problematic for investigators.

Microorganisms play a significant role in the damage induced to DNA. After death, the cell releases nutrients that encourage the growth of these organisms (30). Immunological barriers within the body are no longer physiologically active, thus growth of the microbes is no longer restricted. The microbe digestion can produce acidic byproducts which lead to a decrease in blood pH and a conversion to more anaerobic conditions in bodily fluids (45). Decreases in pH could lead to an increase in the rate of depurination reaction as this reaction is acid catalyzed (35, 46). Physiological stains found within or near soil deposits are subject to microbes found in that environment. The majority of soil microorganisms contain nucleases that induce double strand breaks (DSB) to the structure of DNA, thus causing damage to the samples that are in proximity to them (47). These strand breaks reduce the allelic signal during genotyping especially at larger amplicons.

Another common source of the DNA damage for forensically relevant stains is the effects of weather on the samples. As previously mentioned, the sun's rays contain UVB and UVA radiation, which can produce a variety of lesions to DNA. Humidity and heat have been shown to promote the degradation of nucleic acids by increasing microbial growth and generation of ROS (45, 48). In fecal DNA studies, rainfall has been shown to result in a significant loss of genotyping ability in environmental samples (49). Precipitation can increase the rate of hydrolysis as well as wash away the DNA from the substrate to which it is bound. Samples left in wet conditions for more than 7 days were unable to be genotyped. The length of time the samples were subjected to the rain had more of an influence on the damage induced than the amount of rain itself. This is

another indication of the affect solution chemistry and B-form confirmation in DNA could have on accelerating damage in DNA.

In addition to the adverse effects of weather, many chemical agents are also capable of breaking down nucleic acids and inducing damage to DNA. In terms of chemicals relevant to forensic stains, cleaning agents are quite common and known to modify DNA. Chlorinated bleach was found to have the largest effect on the ability to generate an STR profile in a time-dependent manner (50). Bleach is toxic and able to serve as strong oxidizing agent. Luminol, a common chemical agent used to visualize blood at crime scenes, and soap were found to have no effect on the ability to generate a profile regardless of the surface on which the bloodstain was deposited (51)

Quantification of DNA damages

DNA damage detection assays have been established for many years. Most of these techniques suffer from a lack of sensitivity that could be useful for evaluative environmental samples. The more sensitive techniques often do not provide enough information or accuracy for determination of DNA damage.

A classic technique that is an adequate means of measuring damage to DNA is single cell gel electrophoresis, also known as the comet assay. Briefly, individual cells are lysed in agar, incubated with a glycosylase, then electrophoresis is performed at a high pH and the results are viewed by fluorescent microscopy (52). Damaged DNA appears in the form of a comet with its tail pointing towards the anode due to the formation of single strand breaks. Undamaged cells will retain their DNA because it is still bound by structural proteins. This method has been experimented with as a possible

means of measuring the post mortem interval based on the accumulation of DNA damage; however, the results were not consistent enough for accurate determination (53). Limitations of this method include the need for a viable single cell suspension, overlapping comets and limited information on fragment size (52, 54). This assay is also time consuming and requires specialized lab equipment to be able to view the fluorescent molecules by microscope, which is not ideal.

Another method used in DNA damage quantification is alkaline agarose gel electrophoresis, which also detects single strand breaks. In alkaline gel electrophoresis, samples are run in a high pH environment where the hydrogen bonds between double stranded DNA are denatured and can thus be visualized as single strands (55). Samples are run with standard molecular biology equipment used for gel electrophoresis (56). After electrophoresis, the gel must be soaked in a neutralization solution so that the DNA can be stained. This technique requires large amounts of extracted DNA (up to 200 ng per sample) and analysis time is at least triple of that compared with native agarose gels.

Gas chromatography/mass spectrometry (GC/MS) was used to determine the extent of oxidative damage in bone and tissue of ancient DNA samples (57). GC-MS is often utilized for its ability to detect a multitude of different damaged bases. This technique has the ability to recognize over 25 oxidized and reduced bases in either isolated or cellular DNA (58). However, this method can overestimate oxidative damage as derivatization at high temperatures in the presence of air can lead to the measurement of “artificial” oxidation of undamaged DNA bases (59). Also, at least 30 µg of DNA is required for analysis (60).

Finally, immunoassay techniques have also been used to quantify DNA damage. The slot blot immunoassay has been used to detect UV damage (61). Briefly, denatured DNA is immobilized on a nitrocellulose membrane in slot shaped well. The antibody that selects for the CPDs, anti-T<>T antibody, is incubated in the well, followed by the addition of a secondary enzyme-linked antibody raised against the primary antibody. Chemiluminescence from this reaction can be detected with less than 150 pg of DNA (62). The enzyme-linked immunosorbant assay (ELISA) has also been used to detect CPD formation in DNA (63). The ELISA assay detects unknown antigen associated with UV photoproducts by capture and detection antibodies. The sample antigen binds with the immobilized capture antibodies. Detection antibodies are then employed to complex with the captured antigen. Finally, enzyme linked antibodies are bound to the detection antibody which, after the addition of substrate, results in colorimetric reaction that can be used to visualize the presence of CPDs. The radioimmunoassay has been used as a sensitive means of detecting UV damaged products (64). In a radioimmunoassay, a known quantity of antigen is made radioactive, mixed with a known quantity of antibody and the unknown sample containing an unknown quantity of antigen. Known radioactive antigen competes with the unknown and the ratio indicates the presence of unknown antigen. Antibodies to detect both CPD and oxidative damage products have been developed (65, 66). Cross reactivity with antibodies is a limitation of this method as antibodies often bind to normal guanine bases when using the immunoassay to detect the presence of 8-oxoguanine (67).

Recent DNA damage Detection Methods

More sophisticated methods of damage detection have been developed in recent

years. These new methods include the use of quantitative PCR, advanced chromatographic techniques, and microfluidic devices. Though many improve upon the sensitivity or accuracy measurements, each technique still has its own flaw. No technique has been shown to be applicable for detection in all situations.

Quantitative polymerase chain reaction (qPCR) has been explored as a possible method of damage quantification. As with many PCR assays, this approach only requires nanogram amounts of DNA for analysis. Using different primer sets that are specific to either nuclear or mitochondrial DNA, it is possible to simultaneously compare DNA damage in both these regions (68). The amplification of the target DNA of these regions is compared to the amplification of an internal, shorter sequence that is less likely to be damaged. This ratio is used to determine the amount of damage in the sample. More recently, the long-run rtPCR technique for DNA damage quantification (LORD-Q) method has been examined as a means of DNA quantification. This method is very similar to the previous method of quantification; however, probe sequences greater than 3 kb are employed to increase the sensitivity of detection (69). This was accomplished by addition of a high fidelity polymerase, KAPA2G Fast DNA polymerase, the use of a second-generation fluorescent DNA dye ResoLight, and screening multiple candidate primers (69). While these techniques are very sensitive, the downside is that is they only assay for polymerase stalling damage and are unable to distinguish the different types of damage that may be present in the sample.

The qPCR technique has been applied to forensic science research. A triplex was developed to amplify an STR loci THO1, a 67 bp amplicon nuCSF, and an internal positive control synthetic oligonucleotide to assess PCR inhibition within the assay (70).

As with the above mentioned qPCR strategies, the smaller amplicon is less sensitive to damage and the ratio between THO1 and nuCSF can be used to determine damage to the DNA. The assay was tested on a variety of damaged substrates and the ratio was found to be in good agreement with the extent of damage.

Microfluidic devices have also been examined for use in damage detection. Song and colleagues created an oligonucleotide chip that contains several 20mer fluorescently labeled sequences anchored to a silicon chip (71). This chip-bound DNA is damaged then incubated with a glycoslyase that induces single strand breaks at CPD lesions sites. To detect the fluorescent signal emitted by excitation of the fluorescently labeled sequences, these researchers created a homemade laser detection device to excite the 20mers contained within the chip. A loss of the fluorescent signal is indicative of damage induced and strand break formation. The advantage to this method is that it is highly sensitive due to the ability to detect the strand breaks by laser fluorescence (71). It is also qualitative as different glycosylase enzymes can be used to measure different types of damage (72). The drawback is that the technology is expensive because it requires a complex laser detection system.

Many chromatographic techniques have also been employed for the measurement of DNA damage. Though other HPLC methods can be used, HPLC–ESI-MS/MS is considered the gold standard as analysis by this method yields a higher signal to cell background ratio (73). This technique combines separation by HPLC with the specificity and sensitivity of electrospray ionization mass spectrometry. It is accurate, recognizes a multitude of damaged bases and analysis time is short; however, the disadvantage is that this analysis is expensive and 20 µg of DNA is needed for accurate detection, which is

not often present in DNA found in forensic case samples (58, 60). Also, the accuracy of the instrument is reduced near steady state levels of oxidative damage (58).

PCR Inhibition

Inhibition of the PCR reaction is another complication to consider when evaluating an STR profile. Often, this occurs due to environmental agents present in the sample. This inhibition is difficult to distinguish from degradation as both will cause a decrease in the allelic peaks. Inhibition is the most common cause of amplification failure if sufficient quantities of template are present (74). Inhibitors can bind to the DNA, inhibit polymerase or both.

Many different compounds have been found to inhibit the PCR reaction. Among them, humic compounds are a common source of inhibition which bind to DNA when in contact with soil (75). Humic compounds are fractionated into humic acid (HA) which may chelate the magnesium ions needed for polymerase activity or entrap DNA, making it inaccessible (76, 77). Collagen is also capable of inhibition through binding to the DNA and inhibiting the polymerase (78, 79). Calcium and tanic acid are both inhibitors of *Taq* polymerase. Calcium competes with magnesium for binding sites while tanic acid chelates the magnesium leaving less available for the polymerase (79). Heme, a component of bloodstains, has also been shown to inhibit PCR through binding of *Taq* polymerase; however, DNA extracted by ethanol precipitation is unlikely to contain these compounds due to their solubility (80).

Several methods to overcome PCR inhibition have been proposed and shown to be affective at mitigating the negative effects on STR profiling. A common, and also

simplistic, approach is to dilute the DNA sample in water (81). Though effective, diluting samples of low copy number introduces further complications to profiling as previously discussed. In instances where *Taq* polymerase is being inhibited, concentrations of the polymerase can be increased to overcome the competitive inhibition. Amplification facilitators are also employed to improve the specificity of PCR. Finally, silica based extraction prior to PCR is a robust technique employed to remove a variety of inhibitors. It was found to be more effective than the commonly used phenol/chloroform extraction method and to be applicable to a variety of samples (82, 83).

Base Excision Repair

Understanding the base excision repair (BER) pathway is key to many of the proposed repair methods of DNA lesions as well as DNA damage detection techniques. BER is a cellular mechanism used to remove damaged bases. The primary goal is to repair the sites of lesions in order to maintain genomic integrity within the organism. The first step in repair is recognition of the damaged bases by DNA glycosylases that have the ability to recognize a variety of different lesions. Briefly, these enzymes move along the DNA and cleave the lesion once it is detected, leaving the sugar phosphate backbone intact and creating an abasic (AP) site. This AP site is then incised by glycosylase associated AP lyase activity. The damaged base is removed, strand is nicked and the gap is filled by a polymerase, typically DNA polymerase β in mammals (84). The final process is to seal the remaining nick using DNA ligase.

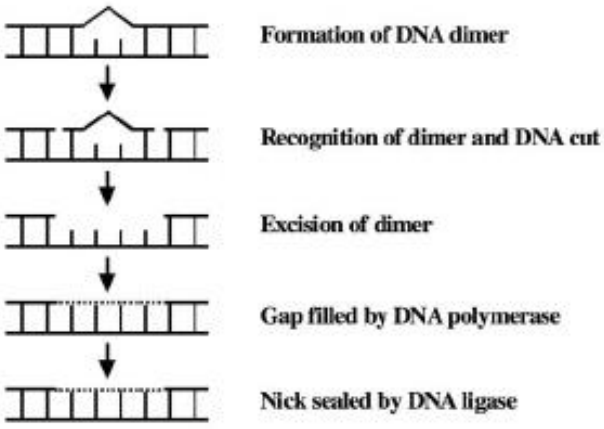

Figure 3 – The Five Enzymatic Steps of the Mammalian BER Pathway. From Sinha & Häder (16).

Glycosylases associated with BER have been well studied for their use in detecting DNA damage. The enzyme T4 endonuclease V is capable of detecting thymine dimers within the primary structure of the DNA. X ray crystallographic analysis of this enzyme reveals that it contains three alpha helices and five reverse loops (85). Before binding to damaged site, the enzyme nonspecifically scans the DNA through electrostatic forces (86, 87). T4 endonuclease V cleaves at the 5' glycosylic bond of the pyrimidine associated with the CPD (88). A sequential AP lyase activity then cleaves the 3' phosphodiester bond leaving α,β-unsaturated aldehyde and a 5'terminal phosphomonoester (89).

FPG (formamidopyrimidine [fapy]-DNA glycosylase) acts in a similar fashion to T4 endonuclease V. FPG recognizes open-ring purines and 8-hydroxypurines within the primary structure of DNA (90). Once the DNA damage is recognized by N-glycosylase activity, the strand is sharply everted through a pocket in the active site (91). It is likely that the bending process provides a clear path for the base out of the base stack by

disrupting the duplex structure (92). The remaining AP site is occupied by hydrophobic residues (91). AP lyase activity carries out β-elimination and strand scission at the 3' AP site. Enzymatic hydrolysis of the phosphodiester backbone results in the formation of a single nucleotide gap at the sequence location previously occupied by an oxidative lesion. Both these enzyme are used to detect damaged bases in damage detection assays. The level of damage is correlated to the amount of strand breaks observed.

Repair/ Recovery of STR Profiles

Repair of the primary structure of DNA has been investigated by a number of forensic scientists. The ability to repair DNA means that there is a greater likelihood that the STR profile can be recovered and serve as evidence in court. Though tremendous efforts have been made, a consistent method of DNA repair of environmentally-damaged samples has not yet been determined.

A popular repair technique among researchers has been the PreCR™ mix developed by New England Biolabs (93). This technique uses a cocktail of different glycosylases and enzymes to remove damaged bases so that polymerase extension can proceed. Incubation time is around 50 minutes before amplification of the sample. Initial reports of this method show very little increase in the ability to generate an STR profile (94). A quantity of at least 50 ng of DNA and the need for additional hands-on time made initial implementation of this technique unappealing. Modifications to the manufacture's protocol have decreased the starting quantity of the reaction to 1 ng which can be analyzed as part of thermocycling (95). The reaction volume and concentration of the reagents were also adjusted to improve upon the manufacturer's protocol. The concentration of enzymes was decreased by one-fourth as compared to the previous

protocol, thus saving resources and improving the ability to recover the profile. Although some success was seen in repairing UV damage, little to no effect was observed when the repair mix was applied to "real world" case samples (94-96).

The Restorase™ enzyme mixture has a similar function to the developed PreCR technique. This repair mix blends repair enzymes with long PCR DNA polymerase to improve STR profiling (97). The Restorase enzyme mix is designed to recover the amplification ability of samples exposed to acid, alkylating agents, heat, and/or light as this damage blocks the progression of the polymerase. The mix is added directly to the PCR reaction but a pre-incubation step is needed before amplification. Restorase was compared directly to the manufacture's protocol for the PreCR reaction and found to recover more of the STR profile; however, the restoration ability of both protocols was marginal compared to no treatment (94). The Restorase mix was used on membrane bound DNA from previous cases involving RFLP and found to have little effect on profile recovery (98).

Instead of repairing the damage to the template, some researchers have opted to either avoid this damaged area or bypass it completely. Translesion polymerases were employed as a means of bypassing these lesion areas during amplification (99). This mechanism requires multiple polymerases in a single reaction to achieve. After *Taq* polymerase stalls at a lesion site, the Y- family translesion polymerase will bind to the template and proceed with extension until it is past the site of damage. These Y- family polymerases are low fidelity and have a larger active site than *Taq* polymerase (100). The spacious active site of Y-family polymerases reduces the stringency of binding allowing damage bases to be recognized by this active site that would otherwise block *Taq*

polymerase. Using a blend of Dpo4 like thermostable Y-family and *Taq* polymerases, researchers were able to significantly increase amplification of UV damaged DNA at the *Alu* locus (99). Further application of this method on different satellite markers and from different damaged sources is being investigated.

Decreasing the size of the amplicons is another way to avoid potentially damaged DNA segments. The "miniSTR" approach reduces the size of all amplicons within the CODIS STR primer regions (101). Larger amplicons have a greater probability to become damaged, so decreasing the size decreases the availability of substrate that could potentially be damaged. This should increase the likelihood of obtaining results when performing CE analysis. Application of this method requires no additional equipment and results are directly comparable to those within the CODIS database (101). Initially, the miniplex contained only three to six different loci; however, it has since been expanded to include non-CODIS loci that increase the power of exclusion (101-103). Larger loci within the CODIS database were not able to be reduced while still functioning as a reliable genetic marker.

Though success has been seen with recovering profiles damaged solely by UV light, environmental samples or samples damaged by multiple agents are still difficult to repair. The miniSTR method has been the most success as it is able to best recover DNA subjected to strand breaks. It is not known however, if a combination of repair enhanced genotyping techniques could further recover a genetic profile or what the major type of damage is within the environmental samples.

This chapter illustrates the complexity of DNA damage and the efforts made to measure and/or repair these lesions. It is apparent this damage negatively affects STR profiling, thus the ability to recover/repair this damage is vital to the recovery of this lost evidence. Further research endeavors into the types of DNA damage found in forensic and environmentally exposed samples will allow for better development of repair strategies that could assist in the recovery of genetic profiles.

CHAPTER 2

UV AND OXIDATIVE DAMAGE DETECTION IN DNA BY GLYCOSYLASE PLUS S1 ENZYME REACTION

Introduction

Genotyping by short tandem repeat profiling is considered to be an extremely valuable source of evidence by forensic scientists. Profiles generated from DNA have led to the determination of innocence and guilt for many cases in the criminal justice system. Though its value is undeniable, DNA as a source of evidence is subject to damage at the scene of the crime, thus compromising its utility for identification. Environmental damage is a known contributor to the loss of a genetic profile and loss of this valuable evidence. Specifically, UV irradiation and oxidative damage by the sun's rays have been known to affect the primary structure of DNA.

UV light can cause strand breaks, base modifications, and photoproduct formation. One of these base modifications is the formation of cyclobutane pyrimidine dimers (CPD) which are predominantly located between adjacent thymine base pairs. UV irradiation saturates the 5,6 double bond between bases which forms a cyclobutane ring (20). Research examining UVC damage to forensically relevant contemporary stains determined that strand breaks are the most likely cause of genetic profile loss and that thymine dimers are less likely to be formed in dehydrated DNA than hydrated DNA due to changes in conformation (40). UVB damage was shown to be more likely to cause allelic dropout while UVA damage had little effect on the ability to generate an STR profile (41).

Oxidative damage is formed after exposure to OH radicals, one-electron oxidants and singlet oxygen reactions (25). This damage can be induced by either ionizing radiation or metabolic processes of aerobic microorganisms (26). The primary form of damage is the alteration of the guanine base to 8-oxo-7,8-dihydroguanine (8-oxoguanine)

which can result in a miscoding of bases during PCR amplification. If this miscoding were to occur in the primer region, the primers may not bind, preventing the polymerase from initiating replication de novo (29).

A commonly used means of measuring the quantity of damage to DNA is single cell gel electrophoresis, also known as the comet assay. Briefly, individual cells are lysed in agar, electrophoresis is performed at a high pH and the results are viewed by fluorescent microscopy (52). Damaged DNA appears in the form of a comet with its tail pointing towards the anode. Limitations of this method are the need for a viable single cell suspension, overlapping comets, and limited information on fragment size (52, 54). This assay is also time consuming and requires specialized lab equipment.

Another method employed is alkaline agarose gel electrophoresis to measure single strand breaks. Alkaline gels work by creating a high pH environment where double stranded DNA is denatured and can thus be visualized as single strands (55). This technique requires large amounts of DNA (up to 200 ng per sample) and the analysis time is at least triple of that seen with native agarose gels. More recent techniques have been proposed to quantify DNA damage including: microfluidic devices, HPLC and fluorescent detection (27). Although the measured quantifications are accurate and sensitive, the downfall of these techniques is that they must be performed with specialized equipment.

The goal of this research was to develop a method of DNA damage detection suited to detecting damage lesions in environmental samples. This information could be useful in determining what types of damage are accounted for in environmental samples

and better construct repair and recovery strategies around this knowledge. The proposed method is inexpensive, requires no specialized equipment and is implemented with less time on the bench compared to an alkaline agarose gel. The idea is to visualize the damage in the same manner as with alkaline gel electrophoresis except using native agarose gel reagents and equipment common to most molecular laboratories. This is accomplished by inducing single strand breaks at the sites of damage using different DNA glycosylases in the same manner as would be done for detection on the alkaline gel. After the initial enzyme digestion, S1 nuclease is used to cleave the DNA opposite these nicked sites in the same tube as the reaction buffer is compatible with both enzymes. Thus, sites of DNA damage are converted to apparent double strand breaks instead of single strand breaks that can be visualized by native gel. True double strand breaks are formed by a single excision event, while apparent double strand breaks here are formed by two separate reactions. Having a buffer compatible with both enzymes means the entire assay can be completed in a single tube which reduces analysis time as well as the loss of DNA between transfers. The strand breaks are visualized as a degradation pattern when run on a native agarose gel as more strand breaks fragment the template leading to those fragments migrating faster on the gel. Thus, the number of apparent double strand breaks visualized is indicative of damage formed due to either oxidation or UV light.

Materials and Methods

Preparation of Synthetic Oligonucleotides

The two synthetic oligonucleotides were synthesized by Integrated DNA technologies (Coralville, IA, USA). The sequences were constructed into a 2056 bp pIDT smart vector with ampicillin resistance. The sequence of the oligo AluSx (appendix A)

was taken from the AluSx locus. *Alu* is a short interspersed element that is found in a high copy number throughout the human genome. The Sx denotes the subfamily of *Alu* that this locus belongs to. The AluSx sequence contains a high number of guanine bases on both strands of the DNA. The other damage oligo, UVC3BPDAM (appendix B), contains two adjacent thymine dimers every three base pairs on opposite strands of the DNA.

The plasmid insert was amplified by polymerase chain reaction using 1 ng of template. The 25 µl reaction mix contained 10 pmol of M13F and M13R primers (IDT), 1x Colorless GoTaq® Flexi Buffer (Promega Corporation, Madison, WI, USA), 2.5 units GoTaq® DNA polymerase (Promega), 1.5 mM $MgCl_2$ (Promega), and 100 µM DNTPS (Promega). PCR was performed with an initial denaturation of 3 minutes at 94°C followed by 25 cycles of denaturation at 94°C for 30 seconds, annealing at 58 °C for 30 seconds, extension at 72°C for 30 seconds, with a final extension of 72°C for 5 minutes.

Multiple samples were amplified then purified using 100K Amicon® ultra centrifugation devices (Millipore Corporation, Billerica, MA, USA). The amplified sample volumes were combined into a single Amicon® filter and centrifuged at 14,000 x g for 5 minutes. Four hundred microliters of sterile water was used to wash the filter containing the DNA sample twice. After each wash, the filter device was centrifuged at 14,000 x g for 5 minutes. After the final wash, the filter was inverted and placed in a new tube, then centrifuged at 1,000 x g for 2 minutes. The eluate containing the purified PCR product was quantified using the Qubit Fluorometer (Life Technologies, Carlsbad, CA, USA).

Damage Assays

Oxidative Damage Assay

Oxidative damage was induced in both genomic DNA and the synthetic control oligonucleotide using methylene blue as a photosensitive producer of singlet oxygen (104). Two hundred nanograms of DNA was incubated in a solution containing 0.03% methylene blue, and 1x PBS in a 20 µl volume in a 0.6 mL tube (Fisher, Norcross GA). The samples were exposed to various amount of light energy supplied by a desk lamp containing a single 60 watt incandescent bulb. This light is absorbed by methylene blue at a wavelength of 550-700 nm (105). The methylene blue acts as a photosensitizer that absorbs the light energy and excites the oxygen molecules in solution. These molecules are then able to participate in singlet oxygen reactions that convert guanine to 8-oxoguanine. The lid of the tubes were left open so that the lamp light would not be blocked. A light source was placed 7 cm above the tubes containing the samples. A petri dish filled with 20 mL of water was placed between the samples and the light source to absorb infrared light that could produce unwanted single strand breaks.

After exposure to lamp light, the volumes contained within each tube were immediately combined into a single 1.5 mL tube (Fisher). Cold absolute ethanol and sodium acetate were added. The tube containing this solution was placed in a -20°C freezer for at least 30 minutes. The DNA was then washed twice with a solution of 70% ethanol and centrifuged at 17,000 g for 5 minutes after each wash. Sterile water was added to re-suspend the DNA and the solution was heated at 56°C for 2 hours as this amount of time was deemed sufficient to resolubilize the DNA.

UVC Damage

Samples were damaged under UV fluorescent light using the UV Stratalinker 1800 (Stratagene, LaJolla, CA, USA). The Stratalinker has five bulbs that deliver light energy at 254 nm. The energy output of the Stratalinker is dependent on the bulb type and will decrease with the age of the bulb. Thus, the amount of energy per minute was determined based on the time it takes to deliver one Joule of energy to the UV sensor contained within the unit. This value was calculated every two weeks to monitor the delivery of UV energy. Each sample to be damaged was placed in a polypropylene microcentrifuge tube, and concentrated to 200 ng/µl. The tubes were placed on their side on the floor of the Stratalinker.

DNA Extraction

DNA extraction was performed using the Qiagen QIAamp Mini Blood Kit (Qiagen, Valencia, CA). When extracting the DNA used as a standard for the damage assays, 200 µl of neat semen was pipetted directly into the 1.5 mL tube. After adding the sample to the tube, a quantity of 400 µl of 1x sterile PBS (Fisher Scientific), 20 µl Qiagen protease and 40 µl of 0.39M DTT were added to each sample and vortexed. Four hundred microliters Buffer AL was combined with the previous solution and mixed quickly to ensure a proper digest of the cell membrane. Samples were incubated at 56°C for 10 minutes. After incubation, 400 µl absolute ethanol was added. The liquid from both tubes was then centrifuged at 6000 x g for 1 minute in a QIAamp Mini spin column using 700 µl aliquots until all of the liquid had passed through the column. The filtrate was discarded and 500 µl Buffer AW1 was added to the column without wetting the rim, then centrifuged at 6000 x g for 1 minute. The filtrate was discarded again and 500 µl

Buffer AW2 was added to the column, then centrifuged at 6000 x g for 3 minutes. The filtrate was removed and the solution centrifuged at 6000 x g for 1 minute to ensure no buffer AW2 remained. Finally, the DNA was eluted by the addition of 50 µL of sterile water, incubated at room temperature for 1 minute, and then centrifuged at 6000 x g for 1 minute.

Quantification

Qubit Fluorometer

The Qubit fluorometer (Life Technologies) uses molecular dyes that will only bind to the target of interest, either DNA, RNA or protein. When bound, fluorescence is emitted that can be quantified on a standard curve generated prior to the quantification of samples. This standard curve is obtained using the two DNA standards included in the Qubit kit. DNA samples were quantified using dsDNA HS kit (Life Technologies). One hundred and ninety-nine microliters of this working solution, containing buffer and the molecular dye, was combined with 1 µL of sample. After addition of the sample, the tubes were incubated at room temperature for two minutes to achieve maximum fluorescent readings. This is the amount of time needed for the molecular dye to bind to the DNA substrate and provide an adequate level of detection.

Enzymatic Digest

Formamidopyrimidine DNA Glycosylase (FPG)

Formamidopyrimidine DNA Glycosylase (New England Biolabs, Ipswich, MA,) is an N-glycosylase with AP-lyase activity which recognizes damaged guanine bases, primarily 8-oxoguanine. Other damaged lesions recognized by this enzyme include 2,6-

diamino-4-hydroxy-5-formamidopyrimidine (FapyGua) and 4,6-diamino-5-formamidopyrimidine (FapyAde) (90). The damaged base is flipped out of the helix by N-glycosylase action and AP-lyase generates a single strand gap by cleavage of the 3' and 5' sites surrounding the AP site. The enzymatic reaction was performed with 2 units of FPG per 200 ng of DNA in 1x NE Buffer 1 (New England Biolabs) (10 mM Bis-Tris-Propane-HCl, 10 mM MgCl2, 1 mM DTT, pH 7 @ 25°C). The solution was incubated over night at 37°C. The reaction was stopped by heat at 65°C for 20 minutes which denatures the enzyme.

Pyrimidine Dimer Glycosylase (T4PDG)

Pyrimidine Dimer Glycosylase (New England Biolabs) recognizes cis-syn CPDs with glycosylase activity and associated AP lyase activity to generate a single strand gap at sites of UV damage. The enzymatic reaction contained 10 units per 200 ng of DNA in 1x T4PDG Reaction Buffer (New England BioLabs) (10 mM Bis-Tris-Propane-HCl, 10 mM $MgCl_2$, 1 mM DTT, pH 7 @ 25°C). The reaction was incubated overnight at 37°C then stopped with heat at 65°C for 20 minutes.

Nt.BstNBI

Nt.BstNBI (New England Biolabs) is an endonuclease that cleaves double stranded DNA substrate to produce single stranded nicks. The naturally occurring enzyme generates these nicks at a 3' recognition site. The reaction contained 10 U/200 ng Nt.BstNBI in 1x NE Buffer 3 (New England Biolabs) (100mM NaCl, 50mM Tris-HCl, 10mM $MgCl_2$,1mM DTT, pH 7.9@25°C). The solution was incubated for 30 minutes at 55°C then stopped by heating at 80°C for 20min. The digested DNA was then purified by

30 K Amicon® ultra centrifugation tubes (Millipore) by combining the volumes of the samples into a filter followed by centrifugation at 3,500 x g for 45 minutes. The use of this size filtration unit instead of the 100k ultra device was used to increase DNA yields. The filter was washed twice with 400 µL of water and spun down each time at 3,500 x g. The filter was then inverted and centrifuged at 1,000 x g to elute the DNA.

S1 Nuclease

S1 nuclease will cleave single stranded DNA opposite the single strand gap, while leaving double stranded DNA intact. The reaction was performed with 5 U/200 ng of S1 nuclease in 1x S1 Nuclease Reaction buffer (Promega) (20mM Tris-HCl (pH 7.5 at 25°C), 0.1mM $ZnCl_2$, 50mM NaCl and 50% (v/v) glycerol). The reaction mixture was incubated one hour at 37°C then stopped by the addition of 2 µL of 0.5 M EDTA and heat at 70°C for 10 minutes.

Glycosylase + S1 assay

An assay to qualitatively and quantitatively measure DNA damage was developed using multiple enzyme digestion and visualized by native agarose gel. In a 10 µl reaction, 100 ng of DNA substrate was first digested with either FPG, to detect oxidative damage, or T4PDG, to detect cyclobutane pyrimidine dimers, in 2 µL of glycylglycine buffer compatible with both enzymatic reactions (0.22M glycylglycine buffer (pH 6.8 at 25°C), 1 M NaCl, 4.3 mM DTT, 27% glycerol in water). The glycylglycine buffer was chosen as it has enzyme activity at pH ranges associated with both the glycosylase reaction and the S1 nuclease reaction. Sodium chloride is added as a cofactor for the enzyme and DTT prevents crosslinking through sulfide bonding that could disrupt activity. After overnight

incubation at 37°C, the reaction was stopped with heat at 65°C for 20 minutes. 5 units of S1 nuclease was then added to the tubes containing the glycosylase digested samples along with 2 µL of the same glycylglycine buffer, 0.001M zinc acetate, pH 4.02 (Amresco LLC Solon, OH), and 0.3M NaCl in a final 20 µL reaction. Zinc acetate and sodium chloride can serve as cofactors for the reaction. Zinc acetate also lowers the pH of the solution to a range more optimal for S1 nuclease digestion. This solution was incubated at 37°C for 1 hour then stopped by addition of 2 µL of 0.5 M EDTA and heat at 70°C for 10 minutes.

Gel Electrophoresis

Native Agarose Gel Preparation

One percent agarose gels were made using 1x TAE (40 mM Tris acetate, 2 mM EDTA) and the appropriate amount of molecular grade agarose (IBI Scientific, Peosta, IA, USA). Samples were prepared in 6x loading buffer (0.25% bromophenol blue, 0.25% xylene cyanol, 30% glycerol in water) then loaded into the wells of the gel. Electrical current was applied to the samples to migrate the DNA through the gel matrix. Either λ HindIII or a 100 bp ladder was used for size comparison. Gels were stained with ethidium bromide (Amresco) or SYBR gold and visualized using a BioRad Gel doc XR+ molecular imager (BioRad Hercules, CA, USA).

Alkaline Agarose Gel Preparation

One percent alkaline gels were made using the appropriate amount of molecular grade Agarose (IBI Scientific) in a gel digest buffer (50 mM NaCl, 1mM EDTA). The gel was soaked in alkaline gel running buffer (30mM NaOH, 1mM EDTA) for at least 30

minutes before the samples were loaded in the gel. The gel must be soaked in sodium hydroxide so that the when run the DNA samples are added to the wells, the DNA will denature during electrophoresis. To each sample an equal amount of Alkaline gel loading buffer (50mM NaOH, 1mM EDTA, 2.5% glycerol, .025% bromocresol green 0.25%) buffer was added. The entire sample was loaded into the wells of the gel. *λ HindIII* was used as a molecular weight marker for all samples due to the inability of the 100 bp ladder to be resolved into discrete bands after being denatured. Electrophoresis was performed at 100V for 2.5 hours. Afterwards, the gel was soaked in neutralization buffer (1 M Tris-HCl pH 7.6, 1.5 M NaCl), and then stained with SYBR gold (Life Technologies) for 1 hour. At this point, the gel was visualized using the BioRad Gel doc XR+ molecular imager.

Average Length Analysis

Gel images were analyzed using Quantity One 1-D Analysis Software Version 4.6.9 (Bio-Rad). Each lane was divided into multiple boxes that covered the fluorescent smear of DNA, so that the volume and molecular weight of each box could be calculated. The molecular weight standards, λHindIII and the 100 bp ladder, were used to generate a dispersion curve based on the distance traveled along the gel. After the molecular weight of each box was calculated, that value was multiplied by the percentage of the volume that the box occupied as part of the entire volume of the fluorescent smear. The final average molecular weight was generated by adding up these percent molecular weight values.

Results and Discussion

Synthetic Oligonucleotide Damage Visualization

The positive control synthetic oligonucleotides were designed incorporating sequences containing base pairs known to be sites susceptible to either oxidative or UV damage. Two oligonucleotides were constructed so that one could serve as a positive control for the formation of 8-oxoguanine and the other for the formation of cyclobutane thymine dimers. The oxidative damage oligonucleotide, AluSX, is 565 bp and contains multiple guanine bases on both sides of the DNA strand (Appendix A). A guanine base is the preferred site of 8-oxoguanine formation, thus the goal was to implement as many guanine pairs as possible into the sequence so that there would be ample sites for the formation of this lesion. The other 565 bp oligonucleotide, UVCDAM, was designed with two consecutive thymine bases alternating every three base pairs on opposite strands, allowing for the measurement of thymine dimer formation (Appendix B). Thymine dimers comprise approximately two-thirds of the total CPD formation and thus are the major alteration to the DNA in the presence of UV radiation while DNA is in the physiological B form (106). Based on the sequence composition, these oligos are able to serve as a positive controls for the glycosylase reactions.

The AluSx oligo was oxidatively damaged using a protocol previously developed involving methylene blue and incandescent desktop light exposure (104). This protocol has been shown to generate 8-oxoguanine damage with few single strand breaks resulting from this damage in the AluSx oligo (Figure 4). DNA samples were digested with FPG then run on alkaline and native gels. Analysis of the digestions on alkaline gel gave

information about the single strand breaks induced by FPG digestion. A native gel was also run to determine that no double strand breaks were present. The enzyme FPG releases the damaged bases and leaves an AP site which is cleaved by an associated AP-lyase activity. Without the addition of this enzyme, few strand breaks were observed. Loss of the high molecular weight band was visualized only in the FPG enzyme digested sample containing both the methylene blue dye and lamp exposure. This indicates, as stated in the literature, both components are required for oxidative damage as methylene blue acts as a photosensitizer which uses the lamp light as energy for the reaction (105). The no light exposure and no dye controls demonstrated that having either light exposure or dye alone is not enough to form oxidative damage. This is evident by the retention of the high molecular weight band even in the presence of the FPG enzyme which would recognize sites of oxidative damage. The no enzyme controls confirmed that no heat, pH, or chemical damage was induced at any point throughout the protocol as this samples contained few single strand breaks. Thus, this protocol was used in future experiments involving the generation of oxidative damage by laboratory methods.

For optimization of the UVCDAM oligo, DNA was subjected to UVC irradiation in a Stratalinker for varying amounts of light energy doses ranging from 0.15 J/cm^2 to 9 J/cm^2 (Figure 5). Afterwards, the enzyme T4PDG was used to cleave the glycosidic bond and phosphodiester bond that surround the pyrimidine dimer. This leaves a nick in the DNA that is visualized as a single strand break during alkaline agarose gel electrophoresis. The alkaline agarose gel confirms the presence of strand breaks that result in a decrease of the average molecular weight with increasing UVC exposure. CPD formation was present after 15 minutes and loss of the high molecular weight band

occurred after one hour. The no T4PDG enzyme controls shows that no strand breaks were formed as a result of UVC irradiation. When visualized on a native agarose gel after T4PDG treatment, the damaged DNA will not show a smear pattern because single strand breaks cannot be visualized by native agarose gels.

Synthetic Oligonucleotide Buffer Optimization

In order for the glycosylase reaction to be combined with S1 nuclease, a reaction buffer needed to be selected in which each of these enzymes could have activity. A buffer containing glycylglycine was chosen due to its ability to maintain pH at ranges corresponding to the enzymes used in this research and its low toxicity to DNA. The optimal pH ranges of the buffer are 2.5-3.8 and 7.5-8.9 correlating to S1 nuclease and glycosylase activity, respectively (107). This buffer was tested alongside with the buffer supplied by New England Biolabs (NEB) to ensure that the enzyme has comparable activity in both buffers. Samples treated with either the FPG or T4PDG enzymes were run on denaturing alkaline agarose gels (Figures 6 and 7). The FPG enzyme produced nearly identical amounts of strand breaks when the reaction was performed with either the glycylglycine buffer or the NEB buffer 1 (Figure 6). The same was true for the T4PDG enzyme in which digestion with either buffer produced a similar smear pattern when visualized on the gel (Figure 7). A smear pattern is indicative of single strand breaks as the high molecular weight DNA is cleaved into smaller fragments that migrate a farther distance towards the anode. No enzyme controls and no damage controls were included in both reactions to ensure that strand breaks were not being formed in samples that were not damaged or were damaged but did not contain the glycosylase enzyme. A slight smear pattern was observed for the oxidative damage samples containing no FPG

enzyme. This indicated that the process of the oxidative damage protocol could have induced a small number of single strand breaks possibly due to heat or strand breaks formed by hydroxyl attack.

Genomic DNA Damage

The same damage protocols were demonstrated with genomic DNA instead of the oligonucleotides. The first step was to extract genomic DNA to use as a standard template for the damage assays (Figure 8). Single strand breaks can be produced during the extraction process that could affect the data when trying to determine strand break formation due to the glycosylase enzyme digestion. Blood stains, buccal swabs, and semen samples were investigated based on DNA yield and amount of single strand breaks. Ultimately, it was determined by alkaline gel electrophoresis that semen produced the highest quantity of DNA and the lowest amount of single strand breaks after extraction. Buccal swabs produced a large amount of DNA but contained single strand breaks, possibly due to enzymatic digestion by salivary enzymes or bacteria in the oral mucosa (108). Blood cells produced few single strand breaks, but yielded low quantities of DNA as only white blood cells contain nuclear DNA. The one caveat of sperm cell extraction was that the samples needed to be digested before being allowed to dry. It is likely that the mechanical stress of dehydration and rehydration is the reason for these observed single strand breaks after dehydration of the sperm samples.

Once the genomic DNA was extracted, the process was similar to that seen with the oligonucleotides. Damage protocols that generated oxidative and UV damage in the oligonucleotide samples were used with the genomic DNA samples. The same single source genomic DNA was subjected to oxidative damage by methylene blue plus light

and UVC damage by UV Stratalinker. The delivery of UV light needed to damage the genomic samples was shorter because the number of single strand breaks formed was higher in the genomic samples. This is likely due to the increased availability of targets as possible damage sites. The increased base pair size of the genomic DNA means there are more base pairs that could become altered or damaged and thus more sites for the glycosylases to cleave single strand breaks.

The damaged DNA was then digested by either FPG or T4PDG in glycylglycine buffer and run on denaturing alkaline agarose gel (Figure 9 and 10). AluSx and UVC3BPDAM were included as positive controls because damage was already demonstrated with these substrates. Genomic samples oxidatively damaged showed decreased average molecular weight with increasing exposure to lamp light when digested with FPG (Figure 9). Double strand break formation was observed in the 30 minute damaged sample signified by a degradation of the high molecular weight band. This is likely due to apparent double strand breaks which would result in a faster migration of the DNA towards the anode as compared to the no damage control. All no enzyme controls showed fewer strand breaks than the damaged, enzyme digested samples.

UV damaged genomic samples were also visualized by alkaline agarose gel (Figure 10). Increasing the delivery of UV light to the samples resulted in an increased loss of the high molecular weight band. No enzyme controls maintained their high molecular weight band as well as the no damage control with enzyme incubation. This indicates that few strand breaks were formed as a result of UV damage or overnight incubation. UVC3BPDAM oligo confirmed the activity of the enzyme and gave a result

similar to those previously seen (Figure 5).

Optimizing the S1 reaction

The S1 reaction was optimized by first generating an appropriate substrate that could serve as a positive control template. The enzyme Nt.BstNBI is an endonuclease that induces a single strand nick four bases after the recognition site GAGTC (109). This enzyme was used to generate a single strand nicked substrate that could be used as a substrate with which the S1 nuclease reaction could be optimized. Different concentrations of Nt.BstNBI were tested to determine the concentration at which single strand break formation began and when over-digestion of the substrate occurred (Figure 11a). Enzyme concentrations of less than 5 units did not produce single strand breaks on the double strand genomic template. After the addition of 30 units, over digestion was observed and double strand breaks began to form as indicated by the native gel (Figure 11b). Ultimately, 10 units of enzyme produced the most reproducible single strand breaks with minimal double strand break formation (Figure 12a). The result is a nicked double strand template of DNA that could serve as substrate for the S1 reaction. A no enzyme control was included to demonstrate that few strand breaks were visualized without the Nt.BstNBI endonuclease.

Using the Nt.BstNBI digested substrate, the optimal concentration of S1 nuclease was calculated based on the visualization of double strand breaks. The DNA substrate previously digested by Nt.BstNBI at a concentration of 10 units was used as a standard DNA substrate for the S1 reaction (Figure 12a). After incubation of multiple samples containing Nt.BstNBI, samples were heated to denature the enzyme. To ensure no buffer remnants interfered with the S1 nuclease reaction, the Nt.BstNBI digested DNA was

purified by Amicon® Ultra 30K centrifugal filter device. The Nt.BstNBI digested substrate could then be further digested with the S1 nuclease to optimize the concentration of enzyme needed for the formation of double strand breaks. Again, increasing enzyme concentrations were used to determine the proper unit amount. A no enzyme negative control was included to confirm that few double strand breaks were present with digestion by the Nt.BstNBI enzyme alone. A concentration of 5 units of S1 nuclease was determined necessary for the visualization of double strand breaks. Concentrations less than this resulted in a retained high molecular weight band when visualized by native agarose gel (Figure 12b).

The S1 reaction was then demonstrated to have activity in the glycylglycine buffer that was compatible with the T4PDG and FPG enzymes (Figure 13). To achieve the same activity seen with the manufacturer's buffer, zinc acetate and sodium chloride was added to the glyclglycine buffer. Zinc acetate serves as a cofactor and also lowers the pH of the reaction (110). S1 activity is pH sensitive and works optimally at a pH of 4.5 (111). Sodium chloride stabilizes helical structures within nucleic acids facilitating the binding of S1 nuclease to the DNA (112). The resulting reaction after addition of these reagents was shown to be comparable to that of the S1 nuclease in buffer supplied by Promega (Figure 13). The no enzyme control again showed that double strand breaks were not occurring before enzyme digestion.

To optimize the incubation time of the S1 nuclease, an enzymatic digest with multiple incubation times and different enzyme conditions was performed (Figure 14). S1 was added to samples digested with Nt.BstNBI and not digested with this enzyme in glyclglycine buffer. The S1 endonuclease reaction was incubated in a water bath for 30

minutes, 60 minutes, or overnight. It was determined that double strand breaks occur as quickly as 30 minutes after incubation with the S1 endonuclease on Nt.BstNBI digested substrate; however, better reproducibility of this digest was observed with a 60 minute incubation time. Without the addition of S1 nuclease, very few double strand breaks were visualized in both Nt.BstNBI digested substrate and double stranded genomic DNA. S1 nuclease was unable to generate double strand breaks without a nicked template to use as substrate. No strand breaks were seen without the addition of either enzyme, indicating that heat and pH buffer did not induce significant damage.

Restriction enzyme + S1 Nuclease Assay

Using the synthetic oligonucleotides as positive damage controls, a novel assay for the measurement of damaged genomic DNA samples was optimized. This assay employs the same DNA glycosylases, FPG and T4PDG, to remove damaged bases; however, to visualize double strand breaks, the enzyme S1 nuclease is used to cleave opposite the single strand nicks just as was seen with the Nt.BstNBI digested substrate.

The reaction involves a two-step enzymatic digestion first by a glycosylase to nick the DNA at sites of damage, then by the S1 nuclease to cleave opposite these sites of damage to generate double stranded breaks that could subsequently be visualized on a native gel. Using the same glycosylase enzymatic reaction that was optimized previously, the genomic standard DNA and the positive control oligos were first digested in the glyclglycine buffer with either the T4PDG or FPG enzyme depending on whether the sample was damaged by UVC irradiation or oxidation respectively. After incubation and abolishment of enzyme activity, reagents for the S1 nuclease reaction were added directly to the tubes containing the glycosylase reaction to reduce the pH and provide cofactors

for S1 activity. The samples were incubated again in the presence and absence of the S1 enzyme. After S1 enzyme activity was terminated by the addition of EDTA and heat, the samples were visualized on a native agarose gel stained with ethidium bromide.

This assay was evaluated on the positive oligonucleotide controls as this DNA has been shown to be damaged by denaturing alkaline agarose gel. Only the oligo samples digested with both the endonuclease and S1 nuclease showed a smear pattern indicative of single strand break formation (Figure 15b). Incubation with the S1 nuclease alone was unable to generate double strand breaks without a single stranded substrate. The single strand breaks generated by either FPG or T4PDG were not visualized on the native agarose gel. Finally, the no enzyme controls show that the heat of the different incubations was not enough to generate double strand breaks in the DNA samples. An alkaline agarose gel was run using the same DNA to show that the results generated by this assay are similar to those seen by glycosylase digestion alone on an alkaline gel (Figure 15a). Enzymes in both assays were able to decrease the average molecular weight of the oligo.

The glycosylase/endonuclease reaction was then taken a step further to demonstrate damage detection in genomic DNA samples (Figure 16 and 18). The positive control oligos were again included as damage detection was already demonstrated in these samples. The oligonucleotide samples could therefore confirm the activity of the enzymes serving as a positive control for the overall reaction.

For the genomic DNA samples, increasing the length of time for damage exposure of the samples corresponded to a decrease in the average molecular weight for

both the samples damaged with UVC irradiation and methylene blue plus lamp light. This was observed in samples that were digested using both the glycosylase and S1 nuclease enzymes. For the FPG plus S1 assay, a small amount of double strand breaks were observed after 30 minutes of exposure to methylene blue plus light when digested with FPG alone (Figure 18). This could be explained by clustered damage as the same DNA visualized by alkaline agarose gel had a degraded high molecular weight band indicative of double strand break formation (Figure 9). Clustered damage is defined as two consecutive strand breaks on opposite strands of DNA that occur within one helical turn and thus form an apparent double strand break (113). Oxidative damage in close proximity could lead to the formation of apparent double strand breaks that are visualized as a smeared band on a native gel and have a degraded high molecular weight band on an alkaline gel. This migration of the high molecular weight band means that the inflicted double strand breaks caused, the now fragmented, high molecular weight DNA to migrate faster resulting in these products to moving further down the gel. The 30 minute damaged –FPG/+S1 lane indicated that single strand breaks could have already been present from the oxidative damage mechanisms as digestion by S1 nuclease alone resulted in a decrease in number average molecular weight (NAMW). NAMW is used to determine the molecular mass of polymers and is defined as the molecular weight of the sample divided by the number of molecules in the sample.

The results were compared to a known damage detection method. Figure 19 shows the gel images of the alkaline agarose gel method and the FPG plus S1 assay. The smear patterns produced are similar showing that this method could be a more sensitive substitution to alkaline agarose gels. Less fluorescence of the glycosylase plus S1 assay

smear patterns could be due to the using ethidum bromide instead of SYBR gold which is a more sensitive stain. This issue could have been resolved by staining with SYBR gold after low signal was observed with ethidum bromide staining.

Similar visualization of damage was seen when samples were incubated with the T4PDG enzyme and S1 nuclease as increasing damage resulted in decreasing molecular weight (Figure 16). The synthetic oligo was again used as a positive control for the overall reaction as it was previously shown to produce double strand breaks by this assay. Only when enzymatically digested with both T4PDG followed by S1 nuclease did the oligo show a diminished high molecular weight band. Nt.BstNBI digested substrate was used as a positive control for the activity of S1 nuclease (Figure 16). When incubated with the S1 enzyme, a smear pattern was observed and without the enzyme few double strand breaks were present. The genomic samples were also incubated in the presence and absence of the different enzymes and were damaged with UVC light with varying amounts of energy delivered. All no damage controls maintained the high molecular weight band, showing no strand break formation and indicating that strand breaks were not formed by the processing of the samples. A decrease in the high molecular weight band was visualized for the T4PDG digested sample of the 0.8 J/cm^2 damage genomic sample and increasingly in the 2.4 J/cm^2 damaged sample. As this level of damage was not seen with the no enzyme, it is likely that apparent double strand breaks were formed as a result of clustered damage induced by the T4PDG digestion as CPD lesions could have formed within one helical turn. The increased delivery of UV light would generate more damage sites that could possibly form within 10 bp. Strand breaks associated with UV damage could have also formed as a decrease of NAMW was seen in sample

digested with only S1 nuclease meaning that this enzyme was able to induce double strand breaks to the single strand breaks formed by this damage. Samples digested by both enzymes T4PDG and S1 showed a dramatic decrease in the average molecular weight indicating that damaged sites were nicked then further digested by S1 nuclease to form double strand breaks. Smear patterns formed by these enzymes when visualized by native gel and those results observed when incubated with T4PDG alone and visualized by alkaline agarose gel both exhibited a pattern of increasing damage with decreasing molecular weight (Figure 17). This demonstrates that using this assay the relative damages could be compared in other samples in an environmental context to determine which component is the most damaging.

The sensitivity of the native gel and alkaline agarose gel was compared to quantitate the differences in the sensitivities of the two methods (Figure 20). Fluorescence could be seen for samples down to 1 ng of DNA when stained with SYBR gold on a native agarose gel. With the same staining process, the lowest amount of DNA needed to visualize fluorescence was 105 ng with the alkaline agarose gel. In terms of a reliable signal, preferred for densitometry analysis, it was determined that 15 ng was needed for the native agarose gel and 150 ng for the alkaline agarose gel. Thus, the native gel technique has ten times greater sensitivity.

Conclusion

Gel electrophoresis is an already established technique for the visualization of DNA and has previously been used in DNA damage studies. Formerly, a high pH environment was required, as seen in the comet assay and denaturing alkaline agarose gel electrophoresis techniques. The glycosylase plus S1 nuclease technique removes the

requirement for a high pH environment because double strand breaks, instead of single strand breaks, are being visualized. Thus, samples can be run on a native agarose gel which is common to most laboratories and there is no need to denature the DNA strands. The resulting gel image of this method is comparable to the alkaline agarose method for both FPG and T4PDG enzyme digestion. The advantage of this method is a smaller quantity of DNA is required for analysis and less time on the bench is needed to complete the assay. The entire reaction is performed inside a single tube which decreases the loss of sample and simplifies analysis.

This technique has downstream applications related to DNA repair and DNA damage studies. Increased sensitivity is useful when studying environmentally damaged DNA as often times only low quantities can be recovered. In terms of DNA repair, the glycosylase plus S1 assay could be used to determine what damage has occurred in a forensic stain and also determine if strand breaks have been reduced due to DNA repair. Information about what type of damage comprises a damaged forensic stain is useful for the creation of competent repair strategies. Ultimately, recognizing and quantifying DNA damage is the first step to the possible recovery of STR profiles lost due to environmental insults.

FIGURES

Time (min)	60	0	60	60	0	60
Dye	-	+	+	-	+	+
FPG	-	-	-	+	+	+
Avg bp	650	590	570	620	580	330

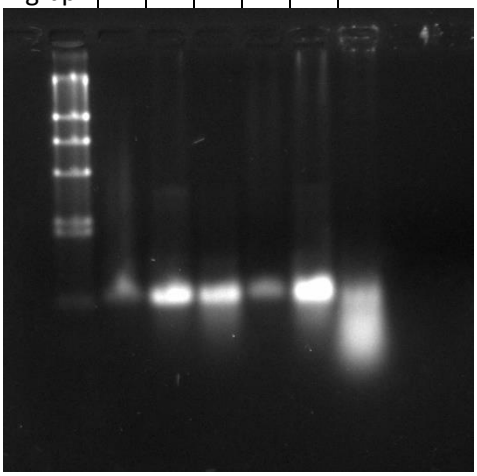

Figure 4. Validation of Oxidative Damage Protocol. Alkaline gel illustrating the ability to damage DNA samples using methylene blue and desk lamp light exposure. Time specifies the length of exposure to lamp light in minutes. + indicates that a certain reagent, either methylene blue or FPG, was added during sample processing and – indicates it was excluded. λ HindIII was used as a ladder for molecular weight evaluation. The 60 minute oxidative damaged DNA was also used in Figure 6.

Damage (J/cm^2)	0	0.15	0.75	2.25	4.5	9	0	0.15	0.75	2.25	4.5	9
T4PDG	+	+	+	+	+	+	-	-	-	-	-	-
Avg bp	535	535	522	444	413	367	520	528	533	540	540	540

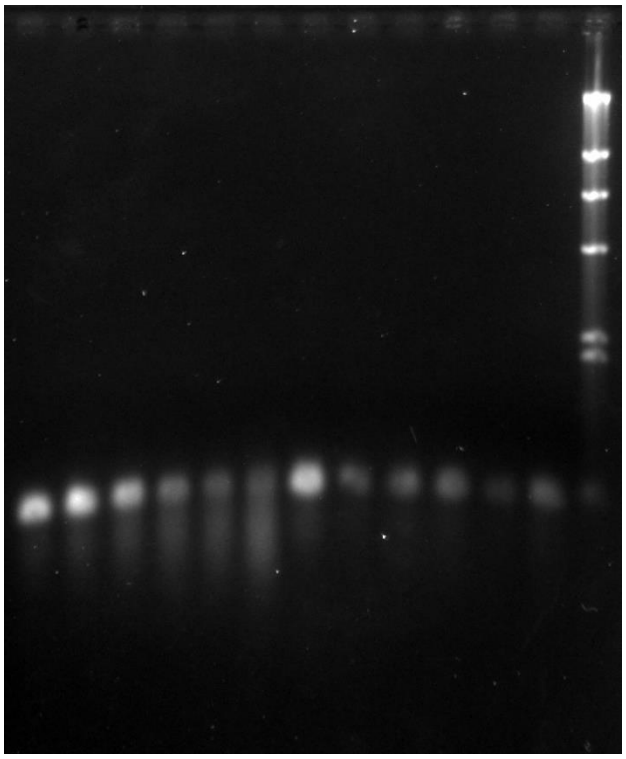

Figure 5. Validation of UVC Damage Protocol. Alkaline gel containing UVCDAM3BP DNA exposed to varying amounts of UVC light damage induced by Stratalinker 1800 and enzymatic digestion by T4PDG. Samples were then visualized with staining in SYBR gold. Once again, λ HindIII was used a reference for molecular weight determination. The DNA damaged for 9 J/cm^2 was selected for use in Figure 7.

Glycylglycine Buffer	-	+	-	+	-	+	-	+
NEB buffer	+	-	+	-	+	-	+	-
Damage (min)	0	0	60	60	0	0	60	60
FPG	+	+	+	+	-	-	-	-
Average bp	562	567	307	307	658	660	592	607

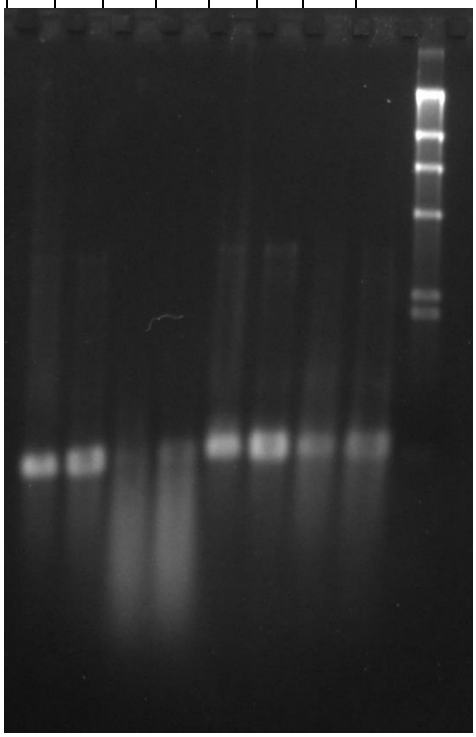

Figure 6. Comparison of Glycylglycine and NEB Buffer reactions with FPG Enzyme. Alkaline gel comparing enzymatic activity between the buffer containing glycylglycine and the buffer supplied by New England Biolabs with the enzyme. Samples were oxidatively damaged by methylene blue plus visible light and digested with FPG. The ladder, λ HindIII, was included as a reference for molecular weight determination.

Glycylglycine Buffer	-	+	-	+	-	+	-	+
NEB buffer	+	-	+	-	+	-	+	-
Damage (J/cm^2)	0	0	9	9	0	0	9	9
T4PDG	+	+	+	+	-	-	-	-
Avg bp	519	540	350	349	527	515	519	523

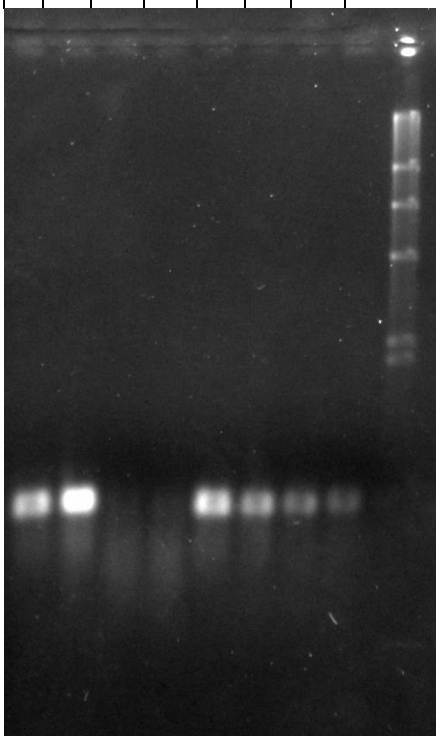

Figure 7. Comparison of Glycylglycine and NEB Buffer reactions with T4PDG Enzyme. Alkaline gel comparing enzymatic activity in the buffer containing glycylglycine and in the buffer supplied by the manufacter (NEB). Samples were exposure to UVC and enzymatic digestion by T4PDG. Damage indicates the length of time the samples were exposed to UVC irradiation. λ HindIII was included for molecular weight determination.

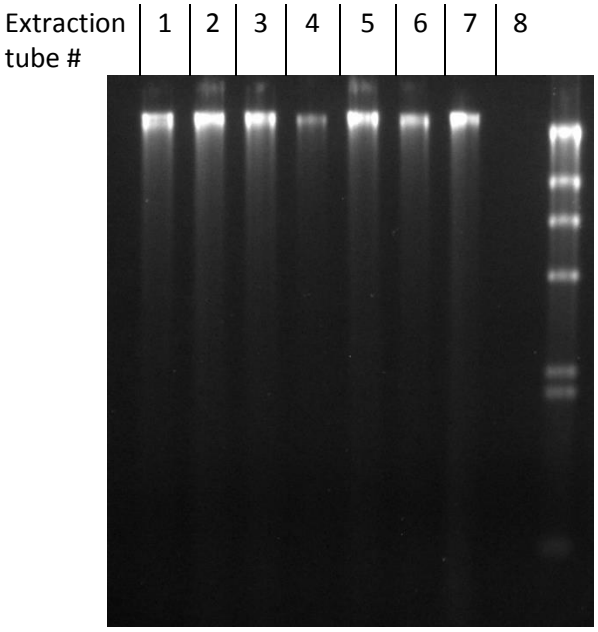

Figure 8. Visualization of Genomic DNA after Extraction. Alkaline gel illustrating that few single strand breaks were seen in genomic DNA samples after Qiagen Extraction. Four hundred microliters of sample was extracted for each tube except 8 which was the extraction blank. λ HindIII was included as a reference for molecular weight determination.

DNA	AluSx				Genomic					
Damage (min)	0	60	0	60	0	15	30	0	15	30
FPG	+	+	-	-	+	+	+	-	-	-
Avg bp	510	410	540	540	11k	4.1k	2.4k	14k	11k	12k

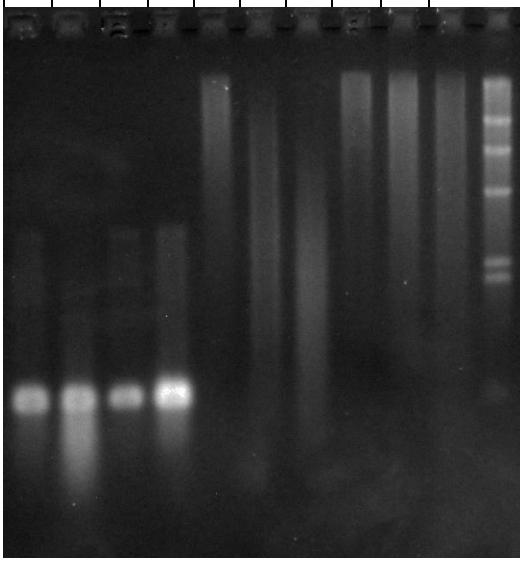

Figure 9. Visualization of Oxidative Damage in Genomic DNA Samples. Alkaline gel illustrating single strand breaks seen in genomic DNA samples after exposure to methylene blue and lamp light for various lengths of time. The oligo AluSx is used to confirm the enzyme activity and serve as a positive control for the reaction. λ HindIII was included as a reference for molecular weight determination. This same DNA samples were incubated simultaneously with samples prepared for Figure 18 for the glycosase plus S1 reaction on native gel.

DNA	UVCDAM3BP				Genomic					
Damage (J/cm^2)	0	6.6	0	6.6	0	0.8	2.4	0	0.8	2.4
T4PDG	+	+	-	-	+	+	+	-	-	-
Avg bp	520	430	520	530	28k	14k	12k	29k	29k	30k

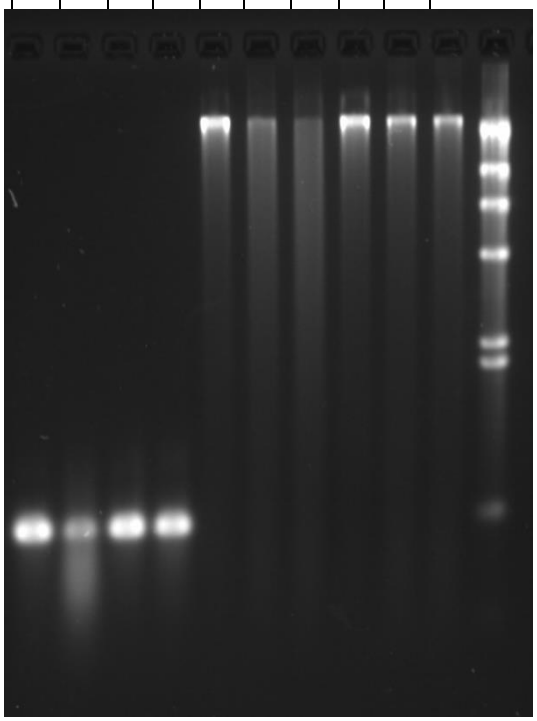

Figure 10. Visualization of UV Damage in Genomic DNA Samples. Alkaline gel illustrating single strand breaks seen in genomic DNA samples after exposure to UVC and enzymatic digestion by T4PDG. The oligo UVCDAM3BP is used as a positive control for enzymatic digestion. λ HindIII is shown as a reference for molecular weight determination. Aliquots of this DNA were incubated simultaneously with samples in Figure 16.

A.

Nt.BstNBI (units)	0	10	5	10	30
Avg bp	27k	8.2k	13k	8.2k	5.5k

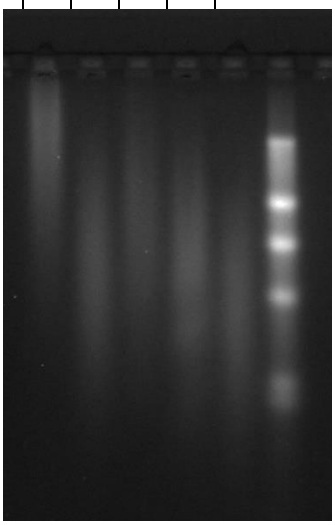

B.

Nt.BstNBI (units)	0	3	5	10	30	x	x	x	x	x	x	x	x
Avg bp	22k	17k	19k	17k	11k	x	x	x	x	x	x	x	x

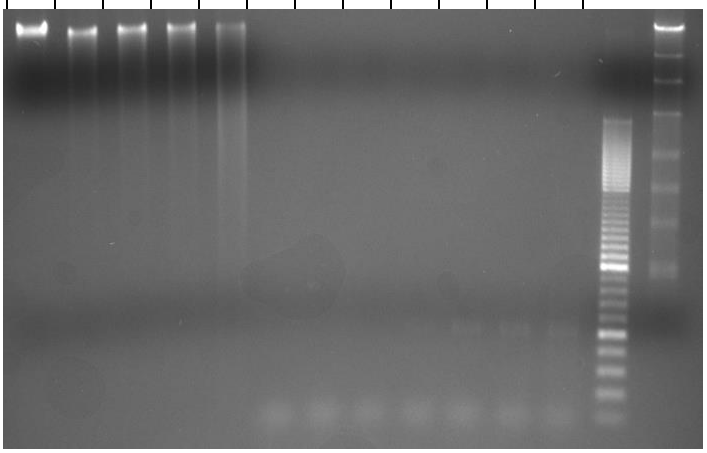

Figure 11. Nt.BstNBI Enzyme Titration. A. Different concentrations of Nt.BstNBI enzyme were incubated with genomic DNA and visualized by alkaline agarose gel detect single strand breaks. **B.** The same DNA was visualized by native gel to determine the presence of DSB. Lanes marked with an "x" were not included in analysis and are unrelated to the experiment. λ HindIII was included as a molecular weight reference.

A)

Nt.BstNBI	+	-
Avg bp	2k	23k

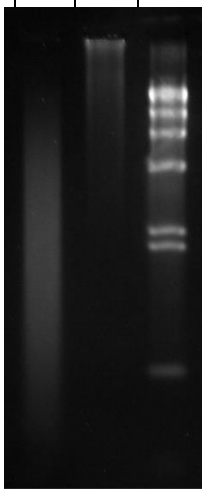

B)

Nt.BstNBI	+	+	+	+	+	+
S1 (units)	-	.3	.6	1	5	10
Avg bp	31k	31k	31k	31k	2.1k	2.0k

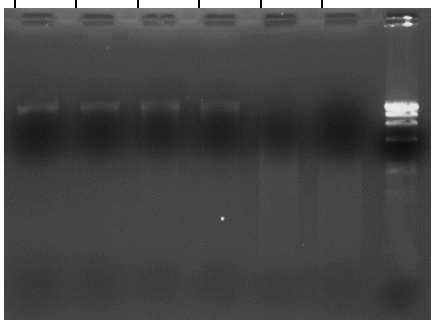

Figure 12. Concentration Optimization of S1 Reaction with Nt.BstNBI Substrate. A. Substrate generated as a positive control for the S1 reaction. The enzyme Nt.BstNBI generates single strand breaks visualized by alkaline gel. S1 cleaves these nicked sites to form double strand breaks. This Nt.BstNBI digested DNA was used as a control for Figures 16 and 18. **B.** A range of enzyme concentrations were tested to determine the activity needed for the visualization of double strand breaks. λ HindIII is shown as a reference for the evaluation of molecular weight.

S1	+	-	+	-
Glycylglycine Buffer	-	-	+	+
S1 Buffer	+	+	-	-
Avg bp	2.4k	13k	2.4k	11k

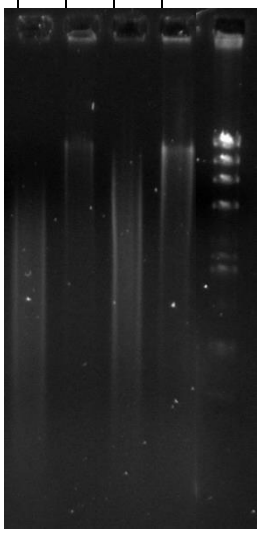

Figure 13. Comparison of Glycylglycine and Promega Buffer Reactions with S1 Endonuclease. Native agarose gel comparing digestion in reactions containing either the glycylglycine buffer or the S1 nuclease reaction buffer supplied by Promega. + indicates which buffer was added to the reaction and whether the S1 enzyme was included in each sample. Nt.BstNBI digested genomic DNA was used as substrate for the reaction. λ HindIII was included as a reference for molecular weight determination.

Nt.BstNBI	+	+	+	-	-	-	+	+	+	-	-	-
S1	+	+	+	+	+	+	-	-	-	-	-	-
incubation (minutes)	30	60	N	30	60	N	30	60	N	30	60	N
Avg bp	3.2k	4.2k	3.0k	42k	37k	46k	54k	25k	23k	31k	28k	37k

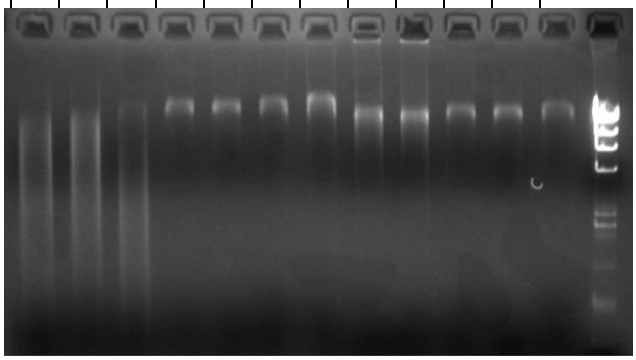

Figure 14. Incubation Optimization for S1 Nuclease. Native agarose gel illustrating double strand breaks in genomic DNA samples after exposure to both Nt.BstNBI and S1 enzymatic digestion. Incubation indicates the time that the samples were incubated at 37°C during S1 enzymatic digestion. N denotes that the samples were left to incubate overnight. λ HindIII was included for molecular weight determination.

A.

DNA template	U	U	A	A	U	U	A	A
Damage (min)			0	60			0	60
Damage (J/cm^2)	0	6.6			0	6.6		
FPG	-	-	+	+	-	-	-	-
T4PDG	+	+	-	-	-	-	-	-
Avg bp	496	395	576	390	543	560	547	594

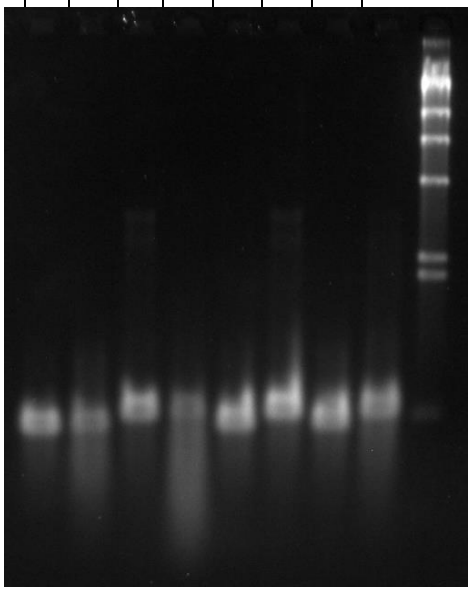

B.

DNA template	U	U	A	A	U	A	U	A	U	A	U	A	U	A	U	A	G	G
Damage (min)			0	60		0		60		0		60		0		60	0	0
Damage (J/cm^2)	0	6.6			0		6.6		0		6.6		0		6.6			
Nt.BstNBI	-	-	-	-	-	-	-	-	-	-	-	-	-	-	-	-	+	+
S1	-	-	-	-	+	+	+	+	+	+	+	+	-	-	-	-	+	-
FPG	-	-	+	+	-	-	-	-	-	+	-	+	-	-	-	-	-	-
T4PDG	+	+	-	-	-	-	-	-	+	-	+	-	-	-	-	-	-	-
Avg bp	440	470	580	580	500	590	500	580	500	580	330	300	440	500	420	460	5.3k	40k

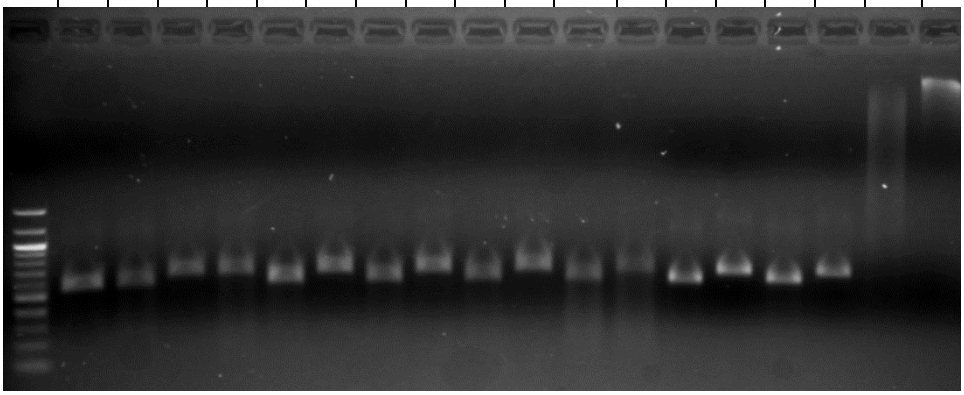

Figure 15. Glycosylase plus S1 Endonuclease Reaction with Positive Control Oligonucleotides. A. Alkaline agarose gel demonstrating single strand breaks induced by the glycosylase alone. This same DNA was visualized on a native gel below. **B**. Native agarose gel illustrating double strand breaks seen in the control oligo samples AluSx (A) and UVCDAM3BP (U), after exposure to either oxidative or UVC damage and enzymatic digestion. Genomic (G) DNA digested with Nt.BstNBI was included as a control for the S1 reaction. 100 bp ladder and λ HindIII was included for molecular weight determination.

DNA	UVCDAM3BP								Genomic														
Damage (J/cm^2)	0	6.6	0	6.6	0	6.6	0	6.6	0	0.8	2.4	0	0.8	2.4	0	0.8	2.4	0	0.8	2.4	0	0	0
T4PDG	+	+	-	-	+	+	-	-	+	+	+	-	-	-	+	+	+	-	-	-	-	-	-
S1	-	-	+	+	+	+	-	-	-	-	-	+	+	+	+	+	+	-	-	-	+	-	-
Nt.BstNBI	-	-	-	-	-	-	-	-	-	-	-	-	-	-	-	-	-	-	-	-	+	+	-
Avg bp	380	415	450	460	420	120	420	440	43k	35k	32k	40k	27k	36k	36k	7k	5k	34k	36k	39k	4.6k	38k	22k

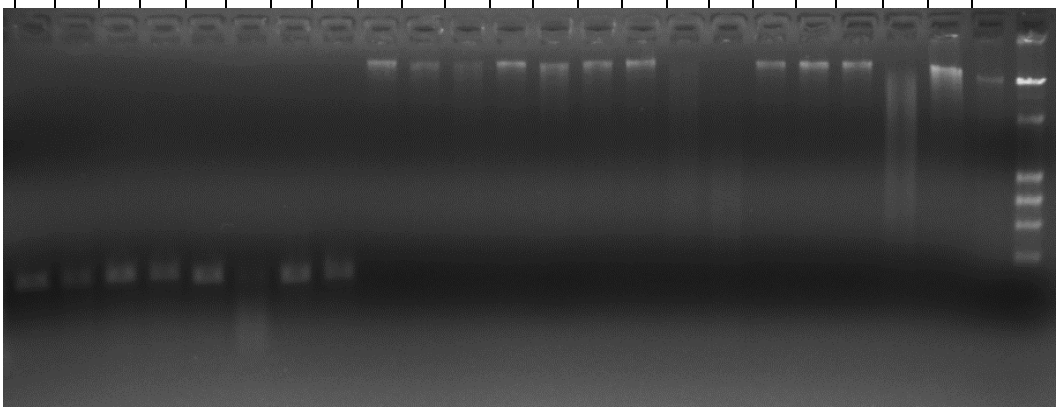

Figure 16. T4PDG plus S1 Endonuclease Reaction with Genomic DNA. Native agarose gel illustrating double strand breaks seen in genomic DNA samples after exposure to both T4PDG and S1 enzymatic digestion. Damage indicates the time that the samples were exposed to UVC irradiation. λ HindIII is shown as a reference for the evaluation of molecular weight.

Damage (J/cm^2)	0	0.8	2.4	0	0.8	2.4
T4PDG	+	+	+	+	+	+
S1	+	+	+	-	-	-
Avg bp	36k	7k	5k	28k	14k	12k

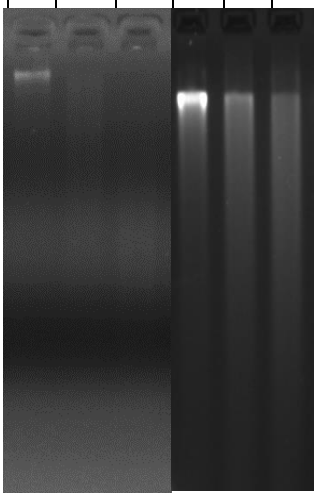

Figure 17. Comparison of T4PDG plus S1 assay to Alkaline Agarose Gel. Figure shows the native agarose gel with T4PDG and S1 enzymatic digestion (left) stained with ethidium bromide and the alkaline agarose gel with T4PDG digestion alone (right) stained with SYBR gold. The same damaged template was used for both methods.

DNA	AluSx								Genomic														
Damage (minutes)	0	60	0	60	0	60	0	60	0	15	30	0	15	30	0	15	30	0	15	30	0	0	0
FPG	+	+	-	-	+	+	-	-	+	+	+	-	-	-	+	+	+	-	-	-	-	-	-
S1	-	-	+	+	+	+	-	-	-	-	-	+	+	+	+	+	+	-	-	-	+	-	-
Nt.BstNBI	-	-	-	-	-	-	-	-	-	-	-	-	-	-	-	-	-	-	-	-	+	+	-
Avg bp	440	300	450	460	460	250	470	460	34k	27k	22k	33k	32k	28k	35k	11k	2.3k	35k	35k	35k	7k	28k	21k

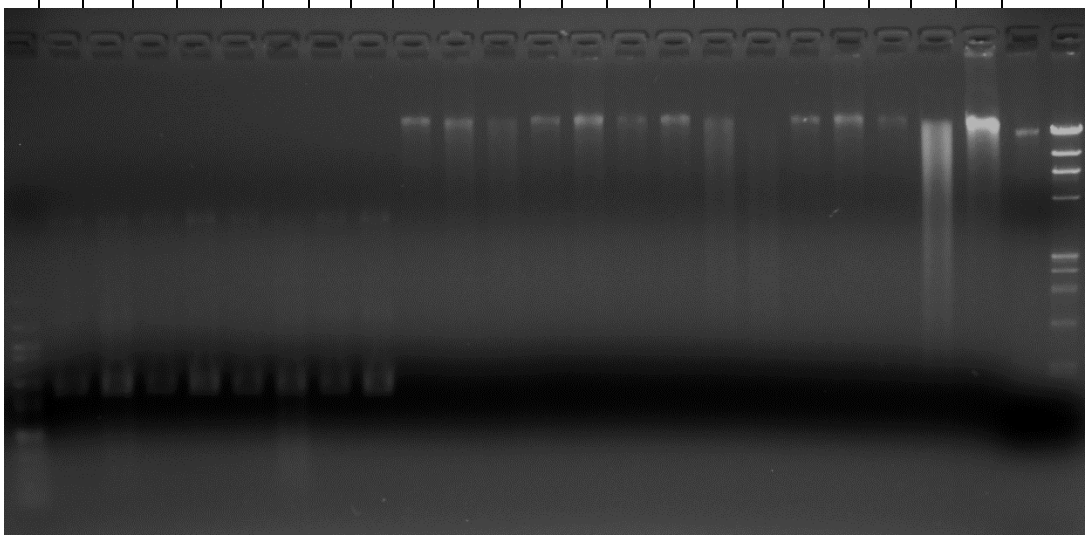

Figure 18. FPG plus S1 Endonuclease Reaction with Genomic DNA. Native agarose gel illustrating double strand breaks seen in genomic DNA samples after exposure to both FPG and S1 enzymatic digestion. Damage denotes the length of time the samples were exposed to lamp light during oxidative damage protocol. Both λ HindIII and a 100 bp ladder were included for molecular weight evaluation.

Damage (minutes)	0	15	30	0	15	30
FPG	+	+	+	+	+	+
S1	+	+	+	-	-	-
Avg bp	35k	11k	2.3k	11k	4.1k	2.4k

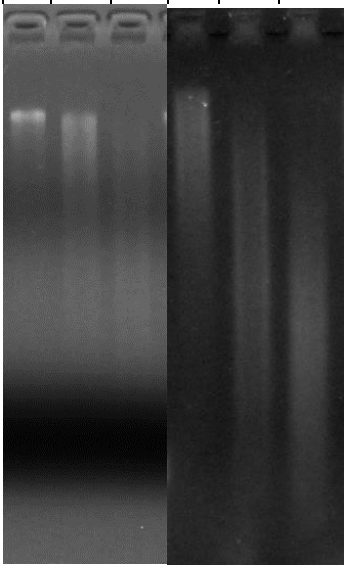

Figure 19. Comparison of FPG plus S1 assay to Alkaline Agarose Gel. Figure shows the native agarose gel with FPG and S1 enzymatic digestion (left) stained with ethidium bromide and the alkaline agarose gel with FPG digestion alone (right) stained with SYBR gold. The same damaged template was used for both methods.

A)

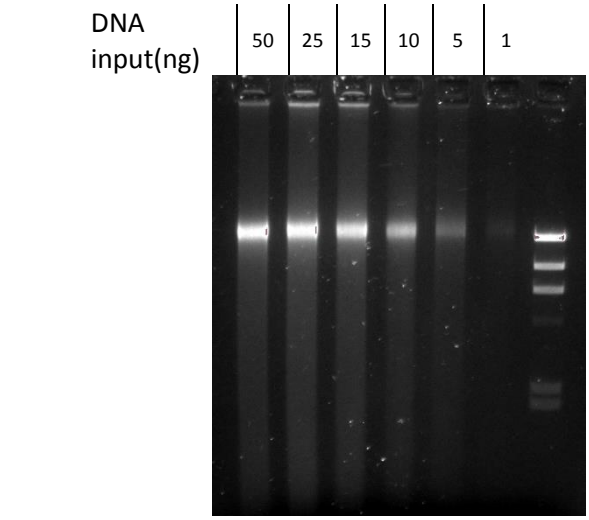

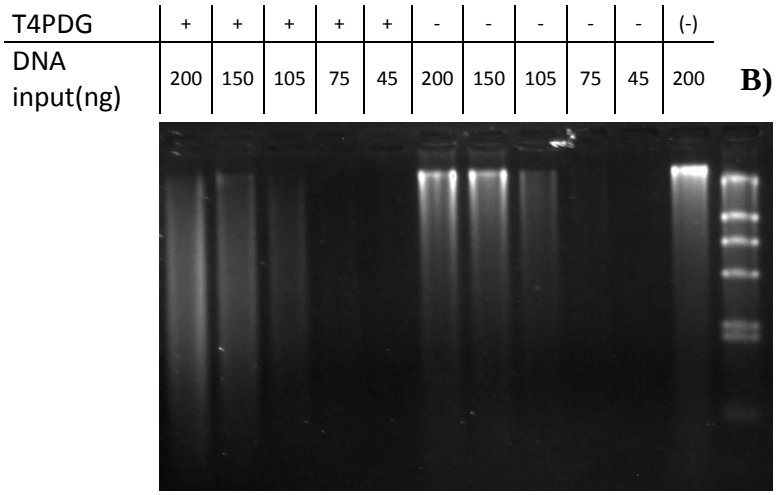

B)

Figure 20. Sensitivity Comparison between Native Gel and Alkaline Agarose Gel. Sensitivity of both the (A) native agarose gel and (B) alkaline agarose gel. Single source genomic DNA was serial diluted across a range of concentrations for both gel techniques. For the alkaline gel, DNA was damaged by delivery of 0.8 J/cm^2 of UVC energy to the samples and digested with T4PDG overnight. The final lane denoted by (-) contains genomic DNA not subjected to UVC irradiation or incubation in a heat bath. Both gels were stained with SYBR gold. λ HindIII was included for molecular weight determination.

Appendix A

AluSx Sequence (290bp)

GCGGGCGGAGGCCGGGCGCGGTGGCTCACGCCTGTAATCCCAGCACTTTGGG
AGGAAGATCACCTGAGGTCAGGAGTTCGAGACCAGCCTGGCCAACATGGTGA
AACCCCGTCTCTACTAAAAATACAAAAATTAGCCGGGCGTGGTGGCGCGCGC
CTGTAATCCCAGCTACTCGGGAGGCTGAGGCAGGAGAATCGCTTGAACCCGG
GAGGCGGAGGTTGCAGTGAGCCGAGATCGCGCCACTGCACTCCAGCCTGGGC
GACAGAGCGAGACTCCGTCTCAAAAAAAA.

Appendix B

UVCDAM3BP Sequence (290bp)

GCAGCAGATTAGAATGTTACAAGGTTATAACCTTATAACATTGCAAGATTCG
AACATTCGAACCTTCGAAGATTCTAAGGTTCGAAGGTTCGAAGATTCGAACG
TTCGAATCTTCTAATATTGCAAGATTCTAAGATTGTAACGTTGCAACCTTGCA
ACATTGCAAGGTTAGAACGTTCTAATATTGGAACATTAGAAGGTTGCAACGT
TCGAATGTTAGAACGTTGCAACGTTGGAACATTGCAATGTTATAATATTGGA
ATCTTAGAACATTGTAACCTTACAGTGTA.

CHAPTER 3

EVALUATION OF ENVIORMENTALLY DAMAGED FORENSIC STAINS

Introduction

Damage to the primary structure of DNA can create many problems for forensic analysis. The primary issue is that this damage can inhibit polymerase extension resulting in a decreased ability to genotype. Few researchers have examined the type of damage that is contained within a contemporary forensic stain exposed to environmental insults. This information could be valuable for the development of strategies to recover the lost profiling data.

It is common to encounter damage to DNA found in environmental samples at a crime scene. McNally et al analyzed forensic case environmentally damaged samples in New York City (114). Their research examined the effect that exposure to the environment has on restriction fragment length polymorphism (RFLP) analysis. The authors first examined the DNA on a native agarose gel to determine if it was of sufficient quality to be evaluated using RFLP. Native gel electrophoresis showed that over half of the 100 samples analyzed contained at least partially degraded DNA. Only DNA that was degraded or partially degraded was evaluated using RFLP. Thus, RFLP profiles were obtained for the majority of samples tested.

Onori et al. exposed bloodstains and tissues to various environmental scenarios such as open air, buried, and wet scenario (44). Bloodstains in a wet environment were the first to exhibit dropout of the allelic profile and decreased quantification; however, allelic dropout was seen in both dry and wet bloodstains as well as the tissue samples within a week of deposition. This indicates when all other factors are similar, blood exhibits degradation of DNA faster than that in the dry state. This is likely due the ability of different damage reagents to act in solution by either diffusion of radicals or hydrolysis

reactions.

Forensic physiological stains are subjected to an array of biotic and abiotic factors that can damage DNA. UV light, heat, humidity, and microorganisms could induce lesions as well as strand breaks to the DNA. After death, the cell releases nutrients that encourage the growth of these microbes, which in turn induce strand breaks (115). Stains deposited near soil sites could also become damaged by soil microorganisms that contain nucleases capable of breaking down the structure of DNA (47).

Atmospheric conditions also impact the intensity of damage on the samples. The sun's rays contain UVB and UVA radiation which can cause in the formation of cyclobutane pyrimidine dimers, 6-4 photoproducts and strand breaks. UV light can also lead to oxidative damage through several mechanisms. UVA light can excite oxygen molecules by photosensitizer reactions, while UVB can cleave cellular water, leading to the formation of reactive oxygen species (ROS) (116). ROS can participate in chemical reactions resulting in the formation of 8-oxo-guanine, the most predominate oxidative lesion (117). These oxidation lesions typically result in base modification rather than inhibition of polymerase extension.

Humidity and heat could also promote the degradation of nucleic acids. Many microbes thrive under these environmental conditions (45). These factors could also increase the nuclease activity of the enzymes leading to increased strand breaks. Moisture due to humidity results in DNA adopting the biological B confirmation rather than the more compact A form characteristic of dehydrated DNA, which contains more base pairs per helical turn and tighter rotational turn angle. B form DNA is more susceptible to UV

damage as the base stacking favors the formation of cyclobutane pyrimidine dimers. Heat can increase the generation of ROS and hydrolytic reactions in solution, resulting in increased oxidative damage and strand breaks (48).

Environmental damage to the primary structure of DNA is common to physiological stains discovered at the scene of the crime. These alterations diminish the ability to recover STR profiles from the DNA. The goal of this research was to detect the level of UV and oxidative damage in "case like" samples that are fully exposed to the environment. Detection of the type and intensity of damage imposed on DNA is the first step in developing a protocol for DNA repair. Using an assay previously developed to detect laboratory induced damage, environmentally damaged samples were quantitatively and qualitatively analyzed on native agarose gels following digestion by glycosylase and S1 nuclease.

Materials and Methods

Environmental Damage

Fresh blood was taken from two unrelated donors by venipuncture. The blood was stored in vials containing 7.2mg EDTA (Fisher Scientific, Norcross GA) and immediately spotted on previously bleached then dried cotton substrate within 24 hours. EDTA is used as an anticoagulant to prevent clotting of the blood. The bleached cotton substrate was stapled to Whatman grade no. 42 filter paper (Fisher Scientific) and an identification card. 20 blood stains containing 50 µl of blood were spotted on each card. The cards containing the blood spots were dried under a fume hood overnight then transported to a secure, outside location.

Samples exposed to the environment were pinned to poster board. The poster board was held down with bricks. Each identification card corresponded to a different time point. Time points ranged from no exposure to 6 months (Table 1). The temperature, humidity, and precipitation were recorded for each week from the Lincoln, NE airport (KLNK). When collecting each time point, a photograph was taken to record the state of the sample, then the sample was placed in a plastic bag as to avoid exposure to water while being stored in the freezer. The samples were stored at -20 °C until DNA extraction.

DNA Extraction

DNA extraction was performed using the QiaAmp DNA Blood Mini Kit (Qiagen, Valencia, CA). Each blood stain was cut into pieces and placed into an extraction tube. After adding the sample to the tube, 400 µl of 1x sterile PBS (Fisher Scientific), and 20 µl Qiagen protease were added to each sample and vortexed. 400 µl Buffer AL was combined with the previous solution and mixed quickly to ensure proper digest of the cell membrane. Samples were incubated at 56°C for 10 minutes. After incubation, 400 µl absolute ethanol was added. The cotton substrate was removed and placed into a new tube containing a spin basket, then centrifuged at 17,000 g for 5 minutes. The liquid from both tubes was then centrifuged at 6000 x g for 1 minute in a QIAamp Mini spin column with 700 µl aliquots until all of the liquid had passed through the column. The filtrate was discarded and 500 µl Buffer AW1 was added to the column without wetting the rim, then centrifuged at 6000 x g for 1 minute. The filtrate was discarded again and 500 µl Buffer AW2 was added to the column, then centrifuged at 6000 x g for 3 minutes. Filtrate was removed and the solution centrifuged at 6000 x g for 1 minute to ensure no buffer AW2

remained. Finally, the DNA was eluted by the addition of 50 µL of sterile water, incubated at room temperature for 1 minute, and then centrifuged at 6000 x g for 1 minute.

In some cases, DNA was extracted from more than one stain for a given time point to increase yield. In this case, the volumes of extracted DNA were combined into a single 30 K Amicon ultra centrifugal filter device (Millipore Corporation, Billerica, MA, USA) followed by centrifugation at 3,500 x g for 45 minutes. The filter was washed twice with 400 µL of water and spun down each time at 3,500 x g for 45 minutes. The filter was then inverted and centrifuged at 1,000 x g to remove the DNA.

qPCR

The DNA from each time point was quantified by qPCR using SYBR green chemistry. The forensic protocol for quantification was developed from Nicklas and Buel (118). A standard curve was obtained using a human DNA standard denoted A314 (Promega, Madison, WI, USA). The eight standard concentrations ranged from 50 ng/µL of DNA to 0.023 ng/µL with a 3x dilution between standards. The master mix contained 0.4 pmoles of *Alu* PCR primers GTCAGGAGATCGAGACCATCCC (forward) and TCCTGCCTCAGCCTCCCAAG (reverse) (Sigma-Aldrich, St. Louis, MO) and 1x SYBR® Select Master Mix (Life Technologies Carlsbad, CA, USA). The total reaction consisted of 8 µL of master mix and 2 µL of DNA template. PCR was performed using the CFX connect Real Time Detection instrument (Bio-Rad, Hercules, CA, USA) with an initial denaturation of 95°C for 2 minutes followed by 30 cycles of 95°C denaturation for 15 seconds, 68°C annealing for 30 seconds, and 72°C extension for 30 seconds. Melt curve analysis was performed starting at 72°C and raising 1°C every 5 seconds until 95°C

was reached. This was performed to determine if multiple products were being formed through during the reaction. Results were visualized using CFX Manager™ Software v3.1 (Bio-Rad).

Glycoslyase plus S1 reaction

In a 10 µl reaction, 15 ng of DNA substrate was first digested with either FPG, to detect oxidative damage, or T4PDG, to detect cyclobutane pyrimidine dimers, in 2 µL of glycyl-glycine buffer compatible with both the glycosylase reaction and the subsequent S1 reaction (.22M glycylglycine buffer (pH 6.8 at 25°C), 1 M NaCl, 4.3 mM DTT, 27% glycerol in water). After overnight incubation at 37°C, the reaction was stopped with heat at 65°C for 20 minutes. In the same tube, 5 units of S1 nuclease were then added to the glycosylase digested samples along with 2 µL of the same glycyl-glycine buffer, 0.001M zinc acetate, pH 4.02 (Amresco LLC Solon, OH), and 0.3M NaCl in a now 20 µL reaction. As previously mentioned, Zinc acetate was added to decrease the pH of the solution which favored S1 nuclease activity. Zinc acetate and sodium chloride were added as cofactors for the reaction. The S1 reaction was incubated at 37°C for 1 hour then stopped by addition of 2 µL of 0.5 M EDTA and heat at 70°C for 10 minutes.

Average Length Analysis

Gel images were analyzed using Quantity One 1-D Analysis Software Version 4.6.9 (Bio-Rad). Each lane was divided into multiple boxes that covered the fluorescent smear of DNA, so that the volume and molecular weight of each box could be calculated. The molecular weight standards, λHindIII and the 100 bp ladder, were used to generate a dispersion curve based on the distance traveled along the gel. After the molecular weight

of each box was calculated, that value was multiplied by the percentage of the volume that the box occupied as part of the entire volume of the fluorescent smear. The final average molecular weight was generated by adding up these percent molecular weight values.

STR analyses

One nanogram of DNA was amplified using a PCR master mix containing multilocus PowerPlex primers. The 25 µL reaction mix consisted of 0.5 units of GoTaq® DNA polymerase (Promega), 1x Colorless GoTaq® Flexi Buffer (Promega), 2.5 mM $MgCl_2$ (Promega), and 250 µM DNTPS (Promega), and 2 µL of PowerPlex primer mix. Thermocycling was performed using the Geneamp PCR system 9700 instrument (Applied Biosystems Foster City, CA, USA). Cycling conditions included: an initial denaturation temperature of 95°C for 5 minutes, 10 cycles of a denaturation at 94°C for 30 seconds, annealing at 60°C for 30 seconds, extension at 70°C for 45 seconds, 22 cycles of a denaturation at 90°C for 30 seconds, annealing at 60°C for 30 seconds, extension at 70°C for 45 seconds, with a final extension of 60°C for 30 minutes.

Post PCR Detection

Post PCR product was detected by injection into the 3130 genetic analyzer (Applied Biosystems). A 0.5 µL aliquot of post PCR product was added to 9 µL of Hi-Di formamide (Life Technologies) and 1 µL of ILS 600 (Promega). ILS serves as a positive control and molecular marker for the base pair length. The plate containing the samples was heated at 95°C for 3 minutes then snap cooled to 4°C for 3 minutes to separate the strands of DNA. The samples were injected into the capillary using the

PPPLEX16_AUG_2011_5V_5S protocol (5s injection, 15 kV, 60°C) with foundation data collection software version 3.0 (Applied Biosystems). Amplicons were separated by electric current through the POP 7 polymer (Life Technologies) and then excited when reaching the laser detection window. The resulting fluorescence was measured in RFU by Genemapper software version 4.0 (Applied Biosystems).

Results and Discussion

Environmental Conditions

Blood stains were exposed to direct sunlight in an unenclosed patio starting in July 2013 in Lincoln, Nebraska. The samples were left uncovered and fully exposed to environmental insults, including moderate to high temperatures, precipitation, and high humidity. Table 1 shows the recorded weather results for each time point. Precipitation first accumulated on the samples within three days of being deposited. High humidity values started around 95% and decreased with time. The average high temperature remained around 27°C for the first month and after six months this value decreased to 19°C. The pictures taken of the bloodstains show fading and color change with time (Figure 21). Rain is likely to be the cause for the fading of the stains as the heme in the blood was washed away from the cotton substrate. Aging of the bloodstains results in oxidation of the iron atoms which changes heme to hematin (119). This could explain the color change from dark red to brown seen in the aged samples.

Quantification of DNA in Environmental Samples

The bloodstains were quantified by qPCR to determine the concentration of DNA (Table 2). The graph below Table 2 shows that the amount of DNA increased from the 0

day time point to the 5 day time point. It is possible that this is the result of jumping PCR. Jumping PCR occurs when the DNA template becomes damaged and fragmented so that these degraded fragments could act as primer for the extension of other PCR products (120). Here, environmental insults could have yielded fragmented DNA, which served as PCR primers. Thus, a potential increase in available primers could lead to an increase in the amplification of DNA during qPCR cycling, resulting in a lower quantification cycle (Cq) that could be interpreted as a higher DNA starting concentration. The Cq denotes the PCR cycle at which the relative fluorescence signal passed the threshold value. Thus, a lower Cq value would correlate to higher amount of starting template. After day 5, there is a sharp decrease in the quantified DNA template. Microorganisms are capable of colonizing a bloodstain within one day and produce nucleases that induce strand breaks (121). This, in combination with the hydrolysis reaction from the moisture of the rain water and possible washing away of the DNA from the cotton substrate, could be possible reasons for the low quantifications seen after five days of environmental exposure. This added hydration could be from rainfall as precipitation more than doubled between the day 5 and day 14 samples.

As was previously determined, the glycosylase plus S1 assay was found to have reliable sensitivity down to 10 ng of DNA (Chapter 2, Figure 20). It was determined that day 0, day 3, and day 5 samples contained sufficient quantities of DNA for analysis with this assay. Because it was suspected that the day 5 samples had an artificially higher concentration due to jumping PCR, a lower concentration for the day 5 sample was estimated using a linear regression line derived from the data points of the day 3 and day 14 samples. This estimated concentration for day 5 was determined to be 2.9 ng/µL.

Experimental Design

After determining DNA concentrations for environmentally damaged samples, the samples were analyzed using both the T4PDG and FPG plus S1 assays to detect both UV and oxidative damage by CPD and 8-oxoguanine presence. The T4PDG plus S1 assay was employed for the determination of UV damage. This assay detects CPDs which are the primary form of damage by UV light when DNA is in the physiological B form confirmation, which is associated with hydrated DNA. Oxidative damage was determined through the formation of 8-oxoguanine. The FPG plus S1 reaction recognizes this lesion. Briefly, the glycosylase enzyme, either FPG or T4PDG, recognizes the damaged base, removes the lesion, and leaves a single strand gap. S1 nuclease then cleaves the strand opposite the single strand nick to produce apparent double strand breaks (DSB) that is visualized by native agarose gel.

For both assays, the no exposure and damaged samples for both control genomic DNA and the positive control oligo were included to validate the glycosylase plus S1 reaction (Figure 22 and 23). The oligo controls contain either a high number of thymine dimer, used in UVC3BPDAM to detect CPDs, or a high number of guanines, used in AluSx to detect 8-oxoguanine. The Nt.BstNBI enzyme with and without S1 digestion was used as a positive control for the activity of the S1 enzyme. Control genomic DNA that was not subjected to either incubation or damage was used as a control to ensure no DSBs are produced during extraction process or dehydration/rehydration of the sample. All samples were incubated in the presence and absence of enzyme. For the environmental samples, this was useful for determining the amount of strand breaks present before the addition of the enzymes. Comparison of the enzyme digested samples

to the no enzyme controls revealed what component of the visualized fluorescent smear is due to oxidative DNA damage because the enzyme digested DNA contained more strand breaks than the no enzyme digest control. A smeared fluorescent pattern indicated the presence of strand breaks, as the smaller fragmented DNA migrated a farther distance towards the anode.

Oxidative Damage in Environmental Samples

Upon visual inspection, the environmentally damaged samples contained increasing strand breaks with increasing days of exposure in the samples without enzyme digestion (Fig. 22, lanes 8-10). With enzyme digestion, a regression of the high molecular weight band and a decrease in the number average molecular weight (NAMW) was observed (Fig. 22, lanes 1-3). NAMW is used to determine the molecular weight of polymers and is defined as the total molecular weight of the sample divided by the number of molecules in the sample. This decrease in NAMW continued with prolonged exposure to the environment. A smear pattern was visualized in the oligo control for only the 60 minute damaged sample digested by FPG (Fig. 22, lane 7). For the genomic controls, 15 minutes of oxidative damage was also demonstrated a reduced NAMW compared to the no enzyme controls (Fig. 22, lane 5). This indicates that the FPG plus S1 reaction functioned as was demonstrated previously (Fig. 18, chapter 2). Degradation of the high molecular weight band in the S1 digested Nt.BstNBI substrate confirmed that the S1 enzyme reaction functioned correctly (Fig. 22, lane 15). A genomic DNA control not subject to incubation was included for comparison to the no enzyme controls to ensure few strand breaks are induced due to heat (Fig. 22, lane 17).

The presence of oxidative lesions with increasing exposure could be due to

various factors. Oxidative damage is a result of the aerobic metabolism of microorganisms. These organisms are known to rapidly colonize biological fluids present outdoors. The added hydration from rainfall could lead to greater diffusion of free radical species, which would allow microorganisms to better access the DNA and produce oxidative lesions. Finally, the UV exposure to the samples could lead to production singlet oxygen or hydroxyl radicals from cleavage of the water molecules surrounding the cell. As stated, hydroxyl radicals can participate in ROS-mediated reactions to produce 8-oxo-guanine.

UV damage in Environmental Samples

For the T4PDG plus S1 reaction, the same environmentally exposed DNA template was used (Figure 23). Again, the genomic DNA and positive control oligo were included for validation of the T4PDG plus S1 reaction. S1 enzyme controls and no incubation genomic DNA were also included as controls for the reaction. Samples were grouped by the presence or absence of enzymes during incubation. No enzyme environmental controls appeared to have the same general smearing pattern as was seen with the no enzyme controls during the FPG plus S1 experiment (Fig. 23, lanes 8-10). A decrease in NAMW was visualized in the day 5 sample incubated with both enzymes when compared to the no enzyme control indicating the presence of CPD damage (Fig. 23, lanes 3 and 10). The genomic DNA control only showed the presence of smearing when exposed to UVC damage and digestion by T4PDG (Fig. 23, lane 5). The damaged, digested oligo control exhibited a slight reduction in NAMW as compared to the no enzyme control (Fig. 23, lane 7). Taken together, the T4PDG enzyme detected CPDs present in the damaged samples. The Nt.BstNBI control confirmed that S1 digestion

results in the formation of double strand breaks (Fig. 23, lane 15). Again, genomic DNA not subjected to incubation was included to compare to the no enzyme controls that underwent incubation (Fig. 23, lane 17).

Number Average Molecular Weight

Densitometry analysis of the samples was performed to quantitate the difference in number average molecular weight (NAMW) between the various samples (Table 3). Comparison of the no enzyme controls to the digested samples indicated that larger differences in NAMW resulted from the cleavage of damage lesions as the environmental exposure increased. FPG plus S1 environmental samples had the largest differences in base pairs, indicating more oxidative damage was observed (Fig. 22, lanes 3 and 10). Large differences in the genomic control samples demonstrated the ability of the FPG and T4PDG enzyme to decrease the average molecular weight by inducing apparent double strand breaks after digestion with both enzymes (Fig. 22 and 23, lanes 5 and 12). Base pair difference was also calculated for the Nt.BstNBI substrate incubated with and without the S1 enzyme (Fig. 22 and 23, lane 15 and 16). A large reduction in average molecular weight was seen with the addition of S1 in both experiments, meaning the enzyme was able to induce apparent DSB to nicked substrate. Differences when comparing the no enzyme, no damage control (Fig. 22 and 23, lane 1) to the enzyme digested, no damage control (Fig. 22 and 23, lane 8) could be due to small changes in DNA migration of the gel or differences in densitometry readings due to specks of fluorescence in the gel.

Based on evaluation of the no enzyme controls of the environmentally exposed DNA, a significant amount of the damage to the samples appears to be caused by double

strand breaks or clustered damage induced by either the processing of the samples or environmental factors. The 0 day, no enzyme control indicated that some level of double strand breaks were induced, likely due to dehydration and rehydration of the samples and possibly due to the extraction process. The NAMW of the no enzyme day 5 sample was around 2,000 bp less than that of the no enzyme day 3 and day 0 samples, meaning that a significant number of strand breaks were induced before the addition of damage detection enzymes. This difference could be due to either hydrolysis as rainfall accumulated between the day 3 and day 5 samples or by microbial digestion of the DNA as these organisms are known to induce double strand breaks. T4PDG and S1 digestion resulted in a decrease of 1,700 bp, meaning that CPD formation was present. The added hydration could have promoted DNA to adopt the physiological B conformation resulting in greater probability of CPD formation. CPDs are typically observed less frequently in the dehydrated A conformation. 8-oxo-guanine was observed at a higher level than CPDs as incubation with FPG and S1 resulted in a reduction of the average molecular weight by 2,200 bp. This does not appear to be unusual as oxidative damage can result from UV light and microbe metabolism (Fig. 22, lanes 1-3). Iron found in heme of the red blood cells could participate in Fenton reactions to generate OH radicals also leading to oxidative damage (122).

STR Profiling

To evaluate the effect the damage induced to the environmentally exposed samples has on the ability to generate a genetic profile, STR profiling was performed (Figure 24). Each sample was analyzed using a 16 loci multiplex containing PowerPlex primers. It was determined that five days of environmental exposure was not enough to

result in allelic drop out. The 0 day, 3 day, and 5 day time points profiles all contained full profiles. Though strand breaks and base modifications were observed in the samples, the damage was not sufficient enough to stall polymerase action. As stated earlier, quantifications of DNA dropped markedly after 5 days from 2.9 ng/ul to 0.09 ng/ul. Thus less template was available for analysis. Only those samples that could be compared to the glycosylase plus S1 assay were evaluated with STR profiling.

Conclusion

DNA damage as a result of environmental insults is a common reason that genetic profiles are unable to be obtained from samples collected at outdoor crime scenes. Repair of these lesions could aid in the recovery of this genetic information. The first step toward repairing environmentally damaged DNA is to detect the type and intensity of damage imposed. In this study, assays were employed that were previously developed to detect damage from 2 types of environmental insults: UV and oxidative. Samples exposed to the environment were evaluated with the glycosylase plus S1 assay to determine the amount of UV and oxidative damage observed with time. Due to low DNA quantification, not all time points could be tested and thus the information gathered was limited; however, differences between the no enzyme control and those incubated with both enzymes demonstrate alterations to the primary structure of DNA by oxidative and UV damage. For both 8-oxoguanine and CPD formation, base alterations were observed within 3 days of being deposited outside. This difference was confirmed through densitometry analysis and determination of the average molecular weight of the degraded DNA. Oxidative damage appeared to be present in a higher quantity than UV damage after 5 days. This finding had yet to be determined in the literature as previous assays to

detect oxidative damage in physiological stains were either concealed by strand breaks induced by other damaging agents or did not possess the sensitivity to detect these lesions.

Strand breaks were observed with increasing environmental exposure in the no enzyme incubated samples. These breaks are likely due to nuclease digestion by microorganisms and hydrolysis reactions. After rainfall at day 3, a greater increase in this damage was observed. Generally, microorganism growth and hydrolysis rates are accelerated in the presence of water. UV and oxidative agents are also capable of inducing single strand breaks to the primary structure of DNA. This is consistent with literature as other studies have found strand breaks to be a major insult in physiological stains (40,41). Strand breaks observed in the 0 day time point are likely due to dehydration and rehydration of the sample.

In addition to strand breaks, hydration could also have played a role in the formation of UV and oxidative DNA damage lesions. An aqueous solution could further enable hydroxyl radicals to access the DNA to form 8-oxoguanine lesions, while also allowing DNA to adopt the B form confirmation. Researchers have proposed that DNA in the B form is more suitable to CPD formation due to the spatial relationship of the bases in this confirmation (40). The high humidity environment could also increase hydration levels that play a role in DNA confirmation as well as diffusion of damaging agents. Heat is likely to increase hydrolytic reactions and the generation of ROS species that participated in oxidative damage and stand break formation.

Taken together, these results demonstrate that UV and oxidative damage is

present in environmentally exposed DNA within a short time span of being deposited outside, but strand breaks appear to account for the majority of damage. Different environmental scenarios must also be assessed to determine the effect on oxidative and UV damage levels. Samples placed in different environment locale, different seasons, and different geographic locations would be useful to determine the level with which these factors affect damage to DNA within physiological stains. Increased knowledge of environmental DNA damage would be useful for forensic investigators at the scene to understand the length of time before DNA is too degraded to generate a profile. It would also benefit forensic researchers studying repair of the DNA and recovery of genetic profiles.

FIGURES

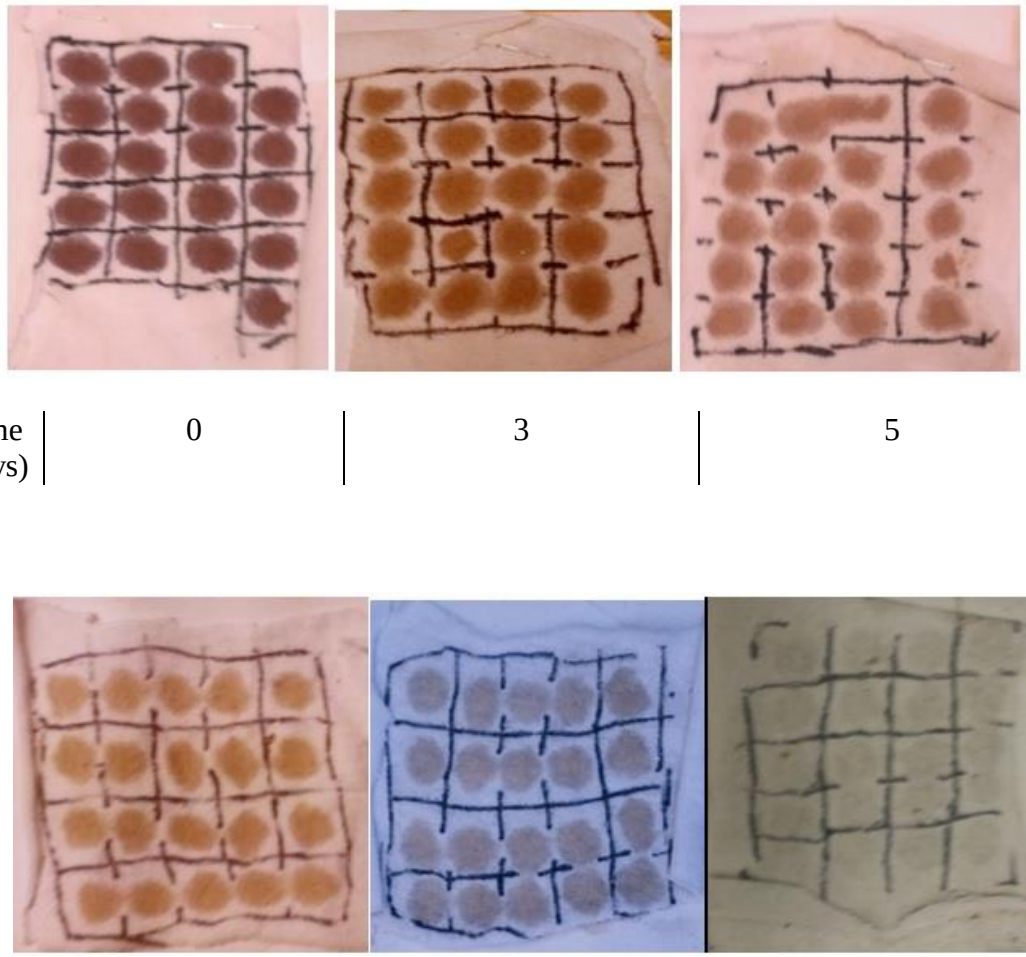

Figure 21. Physical State of Blood Stains. Blood stains subjected to environmental damage for time points ranging from 3 days to 180 days. Pictures were taken after removal from the environment and dried under a fume hood overnight.

Lane number	1	2	3	4	5	6	7		8	9	10	11	12	13	14	15	16	17
Environment Damage (days)	0	3	5	0	0	0	0		0	3	5	0	0	0	0	0	0	0
Damage (minutes)	0	0	0	0	15	0	60		0	0	0	0	15	0	60	0	0	0
FPG	+	+	+	+	+	+	+		-	-	-	-	-	-	-	-	-	-
S1	+	+	+	+	+	+	+		-	-	-	-	-	-	-	+	-	-
Nt.BstNBI	-	-	-	-	-	-	-		-	-	-	-	-	-	-	+	+	-
Avg. MW (bp)	5.3k	4.7k	1.9k	14k	5.4k	610	490		5.8k	6k	4.2k	15k	19k	610	620	10k	16k	18k

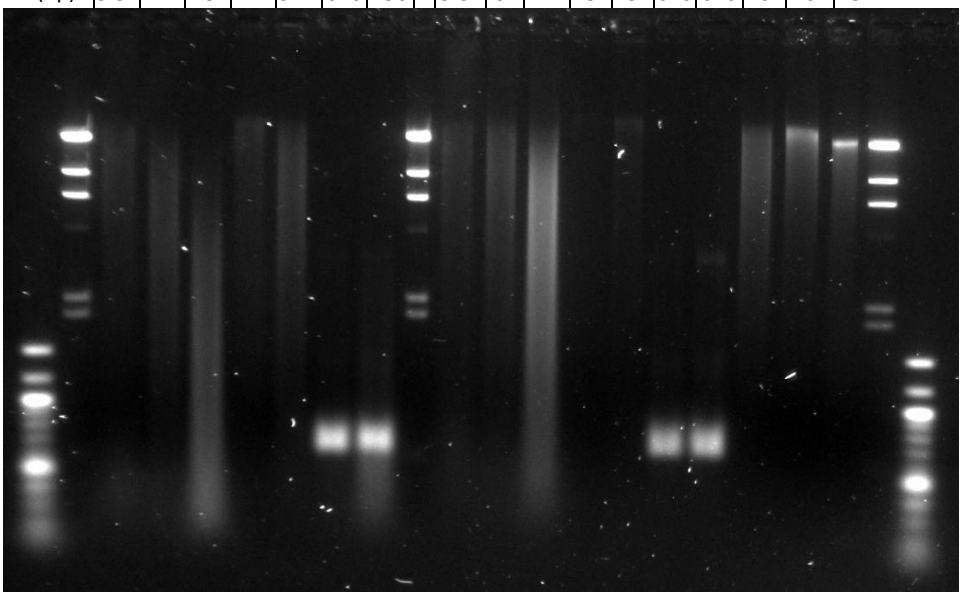

Figure 22. FPG plus S1 Assay to Detect Environmental Oxidative DNA Damage.

Native agarose gel illustrating double strand breaks seen in DNA samples after exposure to environmental conditions. Samples were incubated with FPG and S1 to detect for the presence of oxidative damage. Controls were included to determine enzyme activity. Damage denotes the length of time the samples were exposed to incandescent lamp light during the oxidative damage protocol. Both λ HindIII and a 100 bp ladder were included for molecular weight evaluation.

Lane number	1	2	3	4	5	6	7		8	9	10	11	12	13	14	15	16	17
Environment Damage (days)	0	3	5	0	0	0	0		0	3	5	0	0	0	0	0	0	0
Damage (J/cm^2)	0	0	0	0	0.8	0	6.6		0	0	0	0	0.8	0	6.6	0	0	0
T4PDG	+	+	+	+	+	+	+		-	-	-	-	-	-	-	-	-	-
S1	+	+	+	+	+	+	+		-	-	-	-	-	-	-	+	-	-
Nt.BstNBI	-	-	-	-	-	-	-		-	-	-	-	-	-	-	+	+	-
Avg. MW (bp)	8.3k	7.4k	2.8k	26k	12k	630	610		8.3k	8.8k	4.5k	26k	18k	680	690	12k	25k	19k

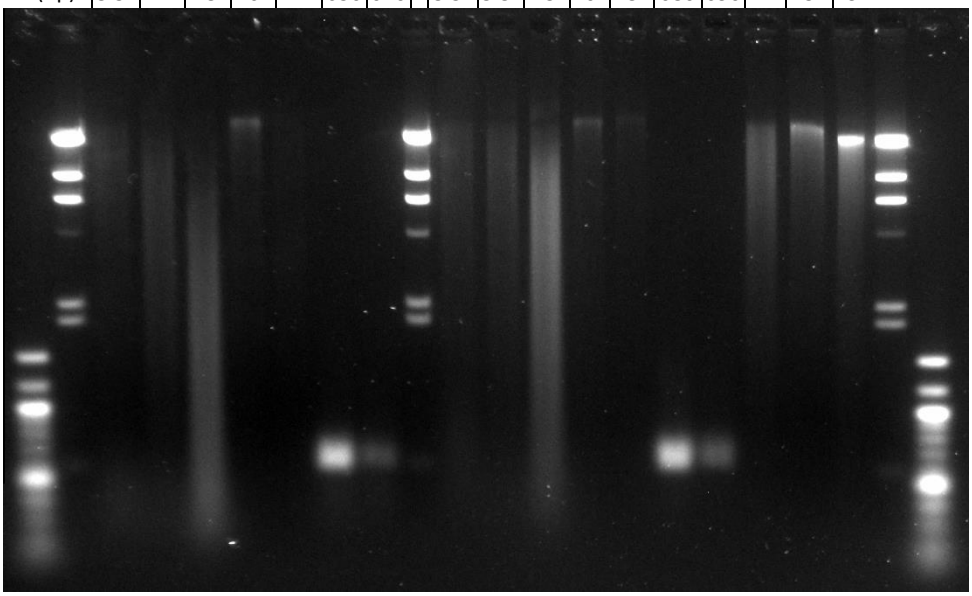

Figure 23. T4PDG plus S1 Assay to Detect Environmental UV DNA Damage Native agarose gel illustrating double strand breaks seen in genomic DNA samples after exposure environmental damage. Samples were digested with T4PDG and S1 to detect for the presence of CPDs. Controls were included to monitor digestion of the different enzymes. Damage denotes the length of energy delivered to samples with the UV Stratalinker. Both λ HindIII and a 100 bp ladder were included for molecular weight evaluation.

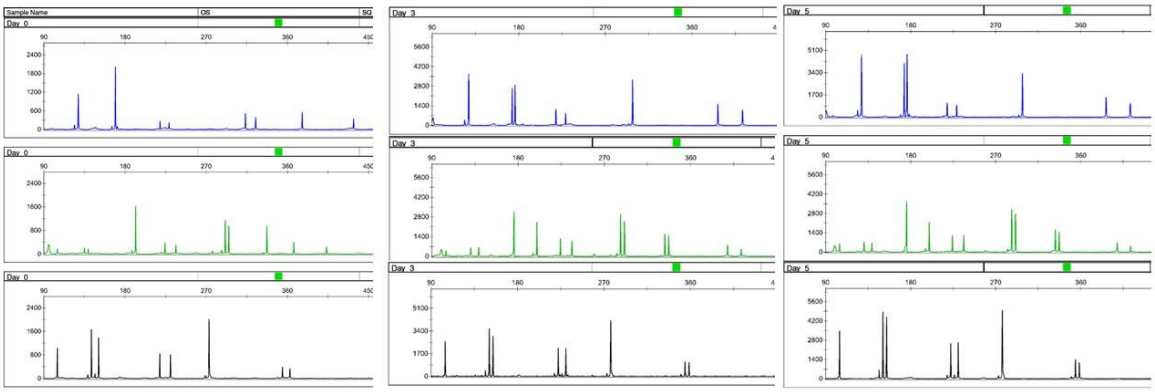

Figure 24. STR Profiles of the Environmental Samples. From the left: day 0, day 3, and day 5 profiles. Because two blood donors were used to generate enough biological material for the study, the day 0 samples originated from a different donor than the day 3 and day 5 samples. Electropherograms were produced by Genemapper software.

TABLES

Samples	Days	Avg high humidity(%)	Average humidity(%)	Precipitation (in)	Days of Rain	Avg high temp (°C)
Day 3	3	92	67	0.72	1	23.5
Day 5	5	95.2	71.2	0.72	1	26.7
Day 14	14	93.6	71.8	1.47	3	27.6
Month 1	31	90.7	69.8	1.83	6	29.0
Month 6	180	85.3	64.1	8.09	26	17.8

Table 1. Weather Information of the Samples Exposed to Environmental Damage. Information includes the average high humidity, average humidity, total precipitation and average high temperature throughout the course of the time point.

Samples	Days	quantification (ng/ul)	volume (ul)	yield (ng)	yield (ng) per stain
Day 0	0	1.27	45	57.15	14.2875
Day 3	3	4.18	45	188.1	47.025
Day 5	5	6.97	44	306.68	76.67
Day 14	14	0.0976	45	4.392	1.098
1 month	31	0.001	47	0.047	0.01175
6 months	180	0.000211	46	0.009706	0.002427

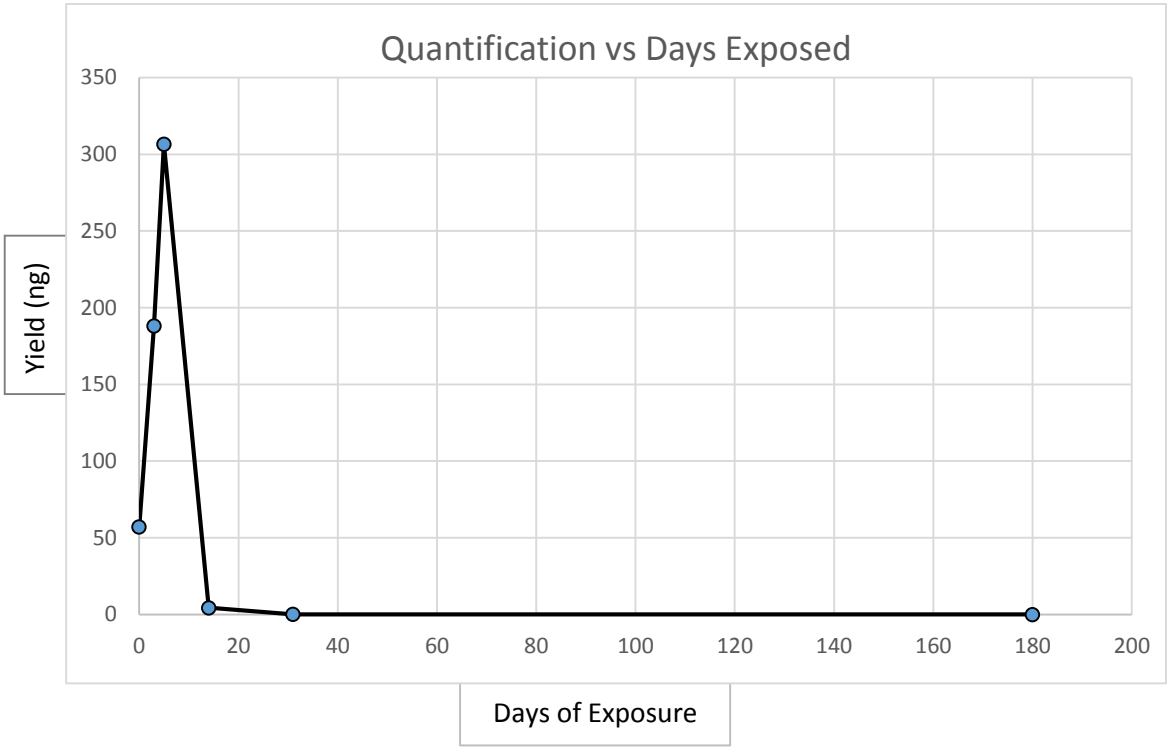

Table 2. Quantification of the Environmentally Exposed Samples by qPCR.

Quantification values generated by CFX manager software. A graph was generated from the total quantity of DNA related to the days of environmental exposure.

	Average bp +FPG	Average bp -FPG	Difference in bp
0 day	5285.4	5825.9	540.6
3 day	4733.4	6022.9	1289.5
5 day	1881.6	4168.6	2287.0
0 min genomic	14320.2	14675.3	355.0
15 min genomic	5446.0	18506.0	13060
0 min Alusx	610.4	611.0	0.58
60 min Alusx	491.2	622.5	131.3

	Average bp +S1	Average bp -S1	Difference in bp
+NtBstNBI	9663.805	16170.72	6506.916

Table 3. Average Molecular Weight Values Associated with the Oxidative Damage Assay. Values were calculated by dividing each fluorescent stain into smaller portions and adding the percentage molecular weight of each division. Information about the molecular weight was generated by quantity one software and the final values were calculated in Microsoft excel.

	Average bp +T4PDG	Average bp -T4PDG	Difference in bp
0 day	8239.2	8285.8	46.6
3 day	7381.1	8861.9	1480.8
5 day	2791.6	4504.3	1712.7
0 min genomic	25639.3	25987.2	347.8
15 min genomic	12252.8	18147.6	5894.8
0 min UVC3BP	627.8	677.2	49.4
60 min UVC3BP	608.5	695.3	86.8

	Average bp +S1	Average bp -S1	Difference in bp
+Nt.BstNBI	12206.5	24518.9	12312.4

Table 4. Average Molecular Weight Values Associated with the UV Damage Assay. Values were calculated by dividing the fluorescent staining into smaller portions and adding the percentage molecular weight of each division. Information about the molecular weight was generated by Quantity One software and the final values were calculated in Microsoft excel.

References

1. Budowle B, Moretti TR, Niezgoda SJ, Brown BL. CODIS and PCR-based short tandem repeat loci: Law enforcement tools. Second european symposium on human identification; Promega Corporation, Madison, Wisconsin; 1998.

2. Guo SW, Thompson EA. Performing the exact test of hardy-weinberg proportion for multiple alleles. Biometrics. 1992:361-72.

3. Jobling MA, Gill P. Encoded evidence: DNA in forensic analysis. Nature Reviews Genetics. 2004;5(10):739-51.

4. Butler JM, Buel E, Crivellente F, McCord BR. Forensic DNA typing by capillary electrophoresis using the ABI prism 310 and 3100 genetic analyzers for STR analysis. Electrophoresis. 2004;25(10-11):1397-412.

5. Gill P, Whitaker J, Flaxman C, Brown N, Buckleton J. An investigation of the rigor of interpretation rules for STRs derived from less than 100 pg of DNA. Forensic Sci Int. 2000 7/24;112(1):17-40.

6. Gill P. Application of low copy number DNA profiling. Croat Med J. 2001;42(3):229-32.

7. Budowle B, Eisenberg AJ, Daal A. Validity of low copy number typing and applications to forensic science. Croat Med J. 2009;50(3):207-17.

8. Whitaker J, Cotton E, Gill P. A comparison of the characteristics of profiles produced with the AMPFlSTR< sup>® SGM plus™ multiplex system for both standard and low copy number (LCN) STR DNA analysis. Forensic Sci Int. 2001;123(2):215-23.

9. van Oorschot RA, Ballantyne KN, Mitchell RJ. Forensic trace DNA: A review. Investig genet. 2010;1(1):14.

10. Dodson M, Michaels ML, Lloyd RS. Unified catalytic mechanism for DNA glycosylases. J Biol Chem. 1994;269:32709-.

11. Van Oorschot RA, Jones MK. DNA fingerprints from fingerprints. NATURE-LONDON-. 1997:767-.

12. Gaines ML, Wojtkiewicz PW, Valentine JA, Brown C. Reduced volume PCR amplification reactions using the AmpFlSTR profiler plus kit. J Forensic Sci. 2002;47(6):1224-37.

13. Juston AC, Frégeau CJ, Fourney RM. STR DNA typing: Increased sensitivity and efficient sample consumption using reduced PCR reaction volumes. J Forensic Sci. 2003;48(5).

14. Smith PJ, Ballantyne J. Simplified Low-Copy-Number DNA analysis by Post-PCR purification. J Forensic Sci. 2007;52(4):820-9.

15. Tevini M. UV-B radiation and ozone depletion. Lewis Publication; 1993.

16. Sinha RP, Häder D. UV-induced DNA damage and repair: A review. Photochemical & Photobiological Sciences. 2002;1(4):225-36.

17. Tornaletti S, Rozek D, Pfeifer GP. The distribution of UV photoproducts along the human p53 gene and its relation to mutations in skin cancer. Oncogene. 1993 Aug;8(8):2051-7.

18. Zavala AG, Morris RT, Wyrick JJ, Smerdon MJ. High-resolution characterization of CPD hotspot formation in human fibroblasts. Nucleic Acids Res. 2014 Jan;42(2):893-905.

19. Lee G, Rabbi M, Clark RL, Marszalek PE. Nanomechanical fingerprints of UV damage to DNA. Small. 2007;3(5):809-13.

20. Breimer LH, Lindahl T. Thymine lesions produced by ionizing radiation in double-stranded DNA. Biochemistry (N Y). 1985;24(15):4018-22.

21. Wang S. Photochemistry and photobiology of nucleic acids. Elsevier; 1976.

22. Labet V, Jorge N, Morell C, Douki T, Grand A, Cadet J, et al. UV-induced formation of the thymine–thymine pyrimidine (6-4) pyrimidone photoproduct–a DFT study of the oxetane intermediate ring opening. Photochemical & Photobiological Sciences. 2013;12(8):1509-16.

23. Mouret S, Baudouin C, Charveron M, Favier A, Cadet J, Douki T. Cyclobutane pyrimidine dimers are predominant DNA lesions in whole human skin exposed to UVA radiation. Proc Natl Acad Sci U S A. 2006 Sep 12;103(37):13765-70.

24. Douki T. UV-induced DNA damage. Biophysical and Physiological Effects of Solar Radiation on Human Skin. 2007:227-69.

25. Cadet J, Douki T, Gasparutto D, Ravanat J. Oxidative damage to DNA: Formation, measurement and biochemical features. Mutation Research/Fundamental and Molecular Mechanisms of Mutagenesis. 2003;531(1):5-23.

26. Alaeddini R, Walsh SJ, Abbas A. Forensic implications of genetic analyses from degraded DNA—a review. Forensic science international: genetics. 2010;4(3):148-57.

27. Cadet J, Douki T, Ravanat J. Oxidatively generated base damage to cellular DNA. Free Radical Biology and Medicine. 2010;49(1):9-21.

28. Cheng KC, Cahill DS, Kasai H, Nishimura S, Loeb LA. 8-hydroxyguanine, an abundant form of oxidative DNA damage, causes G----T and A----C substitutions. J Biol Chem. 1992 Jan 5;267(1):166-72.

29. Sikorsky JA, Primerano DA, Fenger TW, Denvir J. DNA damage reduces< i> taq DNA polymerase fidelity and PCR amplification efficiency. Biochem Biophys Res Commun. 2007;355(2):431-7.

30. Hofreiter M, Serre D, Poinar HN, Kuch M, Pääbo S. Ancient DNA. Nature Reviews Genetics. 2001;2(5):353-9.

31. Fujita S, Steenken S. Pattern of hydroxyl radical addition to uracil and methyl-and carboxyl-substituted uracils. electron transfer of hydroxyl adducts with N, N, N', N'-tetramethyl-p-phenylenediamine and tetranitromethane. J Am Chem Soc. 1981;103(10):2540-5.

32. McNulty JM, Jerkovic B, Bolton PH, Basu AK. Replication inhibition and miscoding properties of DNA templates containing a site-specific cis-thymine glycol or urea residue. Chem Res Toxicol. 1998;11(6):666-73.

33. Balasubramanian B, Pogozelski WK, Tullius TD. DNA strand breaking by the hydroxyl radical is governed by the accessible surface areas of the hydrogen atoms of the DNA backbone. Proc Natl Acad Sci U S A. 1998 Aug 18;95(17):9738-43.

34. Dizdaroglu M, Jaruga P. Mechanisms of free radical-induced damage to DNA. Free Radic Res. 2012;46(4):382-419.

35. Lindahl T, Nyberg B. Rate of depurination of native deoxyribonucleic acid. Biochemistry (N Y). 1972;11(19):3610-8.

36. Lindahl T, Karlstrom O. Heat-induced depyrimidination of deoxyribonucleic acid in neutral solution. Biochemistry (N Y). 1973;12(25):5151-4.

37. Lindahl T. Instability and decay of the primary structure of DNA. Nature. 1993 Apr 22;362(6422):709-15.

38. Marrone A, Ballantyne J. Hydrolysis of DNA and its molecular components in the dry state. Forensic science international: genetics. 2010;4(3):168-77.

39. Ginoza W, Zimm BH. Mechanisms of inactivation of deoxyribonucleic acids by heat. Proc Natl Acad Sci U S A. 1961 May 15;47:639-52.

40. Hall A, Ballantyne J. Characterization of UVC-induced DNA damage in bloodstains: Forensic implications. Analytical and bioanalytical chemistry. 2004;380(1):72-83.

41. Hall A, Sims LM, Ballantyne J. Assessment of DNA damage induced by terrestrial UV irradiation of dried bloodstains: Forensic implications. Forensic Science International: Genetics. 2014;8(1):24-32.

42. McNally L, Shaler RC, Baird M, Balazs I, Kobilinsky L, De Forest P. The effects of environment and substrata on deoxyribonucleic acid (DNA): The use of casework samples from new york city. J Forensic Sci. 1989;34(5):1070-7.

43. Ballantyne J. Assessment and in vitro repair of damaged DNA templates. University of Central Florida, National Center for Forensic Science; 2006.

44. Onori N, Onofri V, Alessandrini F, Buscemi L, Pesaresi M, Turchi C, et al. Post-mortem DNA damage: A comparative study of STRs and SNPs typing efficiency in simulated forensic samples. International congress series; Elsevier; 2006.

45. Gunn A, Pitt SJ. Review paper microbes as forensic indicators. Tropical biomedicine. 2012;29(3):311-30.

46. Zoltewicz JA, Clark DF, Sharpless TW, Grahe G. Kinetics and mechanism of the acid-catalyzed hydrolysis of some purine nucleosides. J Am Chem Soc. 1970;92(6):1741-50.

47. Antheunisse J. DNA decomposition by soil microorganisms. Antonie Van Leeuwenhoek. 1971;37(1):258-9.

48. Bruskov VI, Malakhova LV, Masalimov ZK, Chernikov AV. Heat-induced formation of reactive oxygen species and 8-oxoguanine, a biomarker of damage to DNA. Nucleic Acids Res. 2002 Mar 15;30(6):1354-63.

49. Brinkman TJ, Schwartz MK, Person DK, Pilgrim KL, Hundertmark KJ. Effects of time and rainfall on PCR success using DNA extracted from deer fecal pellets. Conserv Genet. 2010;11(4):1547-52.

50. Harris K, Thacker C, Ballard D, Court DS. The effect of cleaning agents on the DNA analysis of blood stains deposited on different substrates. International congress series; Elsevier; 2006.

51. Gross AM, Harris KA, Kaldun GL. The effect of luminol on presumptive tests and DNA analysis using the polymerase chain reaction. J Forensic Sci. 1999;44:837-40.

52. Collins AR. The comet assay for DNA damage and repair. Mol Biotechnol. 2004;26(3):249-61.

53. Johnson LA, Ferris JA. Analysis of postmortem DNA degradation by single-cell gel electrophoresis. Forensic Sci Int. 2002;126(1):43-7.

54. Olive PL, Banáth JP. The comet assay: A method to measure DNA damage in individual cells. Nature protocols. 2006;1(1):23-9.

55. Sambrook J, Russell DW. Molecular cloning: A laboratory manual. third. Cold pring Harbor Laboratory Press, New York. 2001.

56. Sutherland BM, Bennett PV, Sutherland JC. DNA damage quantitation by alkaline gel electrophoresis. In: DNA Repair Protocols. Springer; 1999. p. 183-202.

57. Hoss M, Jaruga P, Zastawny TH, Dizdaroglu M, Paabo S. DNA damage and DNA sequence retrieval from ancient tissues. Nucleic Acids Res. 1996 Apr 1;24(7):1304-7.

58. Cadet J, Douki T, Ravanat J. Measurement of oxidatively generated base damage in cellular DNA. Mutation Research/Fundamental and Molecular Mechanisms of Mutagenesis. 2011;711(1):3-12.

59. Jenner A, England T, Aruoma O, Halliwell B. Measurement of oxidative DNA damage by gas chromatography–mass spectrometry: Ethanethiol prevents artifactual generation of oxidized DNA bases. Biochem J. 1998;331:365-9.

60. Cadet J, Douki T, Ravanat J. Measurement of oxidatively generated base damage in cellular DNA. Mutation Research/Fundamental and Molecular Mechanisms of Mutagenesis. 2011;711(1):3-12.

61. Muller R, Adamkiewicz J, Rajewsky MF. Immunological detection and quantification of carcinogen-modified DNA components. IARC Sci Publ. 1982;(39)(39):463-79.

62. Walsh PS, Varlaro J, Reynolds R. A rapid chemiluminescent method for quantitation of human DNA. Nucleic Acids Res. 1992 Oct 11;20(19):5061-5.

63. Wani AA, Gibson-D'Ambrosio RE, D'Ambrosio SM. Antibodies to UV irradiated DNA: The monitoring of DNA damage by ELISA and indirect immunofluorescence. Photochem Photobiol. 1984;40(4):465-71.

64. Mitchell DL. Radioimmunoassay of DNA damaged by ultraviolet light. In: Technologies for Detection of DNA Damage and Mutations. Springer; 1996. p. 73-85.

65. Mitchell DL, Meador J, Paniker L, Gasparutto D, Jeffrey WH, Cadet J. Development and application of a novel immunoassay for measuring oxidative DNA damage in the environment. Photochem Photobiol. 2002;75(3):257-65.

66. Sinha RP, Dautz M, Hader D. A simple and efficient method for the quantitative analysis of thymine dimers in cyanobacteria, phytoplankton and macroalgae. Acta Protozool. 2001;40(3):187-96.

67. Cadet J, Douki T, Frelon S, Sauvaigo S, Pouget J, Ravanat J. Assessment of oxidative base damage to isolated and cellular DNA by HPLC-MS/MS measurement< sup> 1, 2. Free Radical Biology and Medicine. 2002;33(4):441-9.

68. Santos JH, Meyer JN, Mandavilli BS, Van Houten B. Quantitative PCR-based measurement of nuclear and mitochondrial DNA damage and repair in mammalian cells. In: DNA Repair Protocols. Springer; 2006. p. 183-99.

69. Lehle S, Hildebrand DG, Merz B, Malak PN, Becker MS, Schmezer P, et al. LORD-Q: A long-run real-time PCR-based DNA-damage quantification method for nuclear and mitochondrial genome analysis. Nucleic Acids Res. 2014 Apr;42(6):e41.

70. Swango KL, Timken MD, Chong MD, Buoncristiani MR. A quantitative PCR assay for the assessment of DNA degradation in forensic samples. Forensic Sci Int. 2006;158(1):14-26.

71. Pal S, Kim MJ, Choo J, Kang SH, Lee K, Song JM. Quantitation of ultraviolet-induced single-strand breaks using oligonucleotide chip. Anal Chim Acta. 2008;622(1):195-200.

72. Ki HA, Kim MJ, Pal S, Song JM. Oligonucleotide chip assay for quantification of gamma ray-induced single strand breaks. J Pharm Biomed Anal. 2009;49(2):562-6.

73. Cadet J, Poulsen H. Measurement of oxidatively generated base damage in cellular DNA and urine. Free Radical Biology and Medicine. 2010;48(11):1457-9.

74. Alaeddini R. Forensic implications of PCR inhibition—a review. Forensic Science International: Genetics. 2012;6(3):297-305.

75. Sutlovic D, Gamulin S, Definis-Gojanovic M, Gugic D, Andjelinovic S. Interaction of humic acids with human DNA: Proposed mechanisms and kinetics. Electrophoresis. 2008;29(7):1467-72.

76. Tsai YL, Olson BH. Detection of low numbers of bacterial cells in soils and sediments by polymerase chain reaction. Appl Environ Microbiol. 1992 Feb;58(2):754-7.

77. Poinar HN, Hofreiter M, Spaulding WG, Martin PS, Stankiewicz BA, Bland H, et al. Molecular coproscopy: Dung and diet of the extinct ground sloth nothrotheriops shastensis. Science. 1998 Jul 17;281(5375):402-6.

78. Scholz M, Giddings I, Pusch CM. A polymerase chain reaction inhibitor of ancient hard and soft tissue DNA extracts is determined as human collagen type I. Anal Biochem. 1998;259(2):283-6.

79. McCord B, Opel K, Funes M, Zoppis S, Meadows Jantz L. An investigation of the effect of DNA degradation and inhibition on PCR amplification of single source and mixed forensic samples. NIJ Grant Summary, 2011-07-10. 2011.

80. Akane A, Matsubara K, Nakamura H, Takahashi S, Kimura K. Identification of the heme compound copurified with deoxyribonucleic acid (DNA) from bloodstains, a major inhibitor of polymerase chain reaction (PCR) amplification. J Forensic Sci. 1994;39:362-.

81. Alonso A, Andelinovic S, Martín P, Sutlovic D, Erceg I, Huffine E, et al. DNA typing from skeletal remains: Evaluation of multiplex and megaplex STR systems on DNA isolated from bone and teeth samples. Croat Med J. 2001;42(3):260-6.

82. Boddinghaus B, Wichelhaus TA, Brade V, Bittner T. Removal of PCR inhibitors by silica membranes: Evaluating the amplicor mycobacterium tuberculosis kit. J Clin Microbiol. 2001 Oct;39(10):3750-2.

83. Parsons T. Highly effective DNA extraction method for nuclear short tandem repeat testing of skeletal remains from mass graves. Croat Med J. 2007;48:478-85.

84. Beard WA, Wilson SH. Structure and mechanism of DNA polymerase β. Chem Rev. 2006;106(2):361-82.

85. Morikawa K, Matsumoto O, Tsujimoto M, Katayanagi K, Ariyoshi M, Doi T, et al. X-ray structure of T4 endonuclease V: An excision repair enzyme specific for a pyrimidine dimer. Science. 1992;256(5056):523-6.

86. Radany EH, Friedberg EC. A pyrimidine dimer–DNA glycosylase activity associated with the v gene product of bacteriophage T4. . 1980.

87. Dodson M, Lloyd R. Structure-function studies of the T4 endonuclease V repair enzyme. Mutat Res /DNA Repair. 1989;218(2):49-65.

88. Schrock RD,3rd, Lloyd RS. Reductive methylation of the amino terminus of endonuclease V eradicates catalytic activities. evidence for an essential role of the amino terminus in the chemical mechanisms of catalysis. J Biol Chem. 1991 Sep 15;266(26):17631-9.

89. Weiss B, Grossman L. Phosphodiesterases involved in DNA repair. Advances in Enzymology and Related Areas of Molecular Biology, Volume 60. 1987:1-34.

90. Boiteux S, Gajewski E, Laval J, Dizdaroglu M. Substrate specificity of the escherichia coli fpg protein formamidopyrimidine-DNA glycosylase: Excision of purine lesions in DNA produced by ionizing radiation or photosensitization. Biochemistry (N Y). 1992;31(1):106-10.

91. Zharkov DO, Grollman AP. The DNA trackwalkers: Principles of lesion search and recognition by DNA glycosylases. Mutation Research/Fundamental and Molecular Mechanisms of Mutagenesis. 2005;577(1):24-54.

92. Friedman JI, Stivers JT. Detection of damaged DNA bases by DNA glycosylase enzymes. Biochemistry (N Y). 2010;49(24):4957-67.

93. New England Biolabs I. PreCR repair mix. Technical Bulletin for PreCR Repair Mix. 2007.

94. Westen AA, Sijen T. Degraded DNA sample analysis using DNA repair enzymes, mini-STRs and (tri-allelic) SNPs. Forensic Science International: Genetics Supplement Series. 2009;2(1):505-7.

95. Diegoli TM, Farr M, Cromartie C, Coble MD, Bille TW. An optimized protocol for forensic application of the PreCR™ repair mix to multiplex STR amplification of UV-damaged DNA. Forensic Science International: Genetics. 2012 7;6(4):498-503.

96. Ambers A, Turnbough M, Benjamin R, King J, Budowle B. Assessment of the role of DNA repair in damaged forensic samples. Int J Legal Med. 2014:1-9.

97. Walker C, Mueller E, Buntaine B, Boedeker B, Kayser K. Restorase®: A novel DNA polymerase blend that repairs damaged DNA. Life Science. 2004;July(4-5):18.

98. Steadman SA, McDonald JD, Andrews JS, Watson ND. Recovery and STR amplification of DNA from RFLP membranes*. J Forensic Sci. 2008;53(2):349-58.

99. McDonald JP, Hall A, Gasparutto D, Cadet J, Ballantyne J, Woodgate R. Novel thermostable Y-family polymerases: Applications for the PCR amplification of damaged or ancient DNAs. Nucleic Acids Res. 2006 Feb 18;34(4):1102-11.

100. Sale JE, Lehmann AR, Woodgate R. Y-family DNA polymerases and their role in tolerance of cellular DNA damage. Nature Reviews Molecular Cell Biology. 2012;13(3):141-52.

101. Butler JM, Shen Y, McCord BR. The development of reduced size STR amplicons as tools for analysis of degraded DNA. J Forensic Sci. 2003;48(5):1054-64.

102. Coble M, Hill C, Vallone P, Butler J. Characterization and performance of new MiniSTR loci for typing degraded samples. International congress series; Elsevier; 2006.

103. Decorte R, Liu CF, Vanderheyden N, Cassiman J. Development of a novel miniSTR multiplex assay for typing degraded DNA samples. Forensic Science International: Genetics Supplement Series. 2008;1(1):112-4.

104. Floyd R, West M, Eneff K, Schneider J. Methylene blue plus light mediates 8-hydroxyguanine formation in DNA. Arch Biochem Biophys. 1989;273(1):106-11.

105. DeRosa MC, Crutchley RJ. Photosensitized singlet oxygen and its applications. Coord Chem Rev. 2002;233:351-71.

106. Friedberg EC, Walker GC, Siede W. DNA repair and mutagenesis. American Society for Microbiology (ASM); 1995.

107. O'Neil MJ. The merck index: An encyclopedia of chemicals, drugs, and biologicals. RSC Publishing; 2013.

108. Milne E, van Bockxmeer FM, Robertson L, Brisbane JM, Ashton LJ, Scott RJ, et al. Buccal DNA collection: Comparison of buccal swabs with FTA cards. Cancer Epidemiol Biomarkers Prev. 2006 Apr;15(4):816-9.

109. Morgan RD, Calvet C, Demeter M, Agra R, Kong H. Characterization of the specific DNA nicking activity of restriction endonuclease N.BstNBI. Biol Chem. 2000 Nov;381(11):1123-5.

110. Wiegand RC, Godson GN, Radding CM. Specificity of the S1 nuclease from aspergillus oryzae. J Biol Chem. 1975 Nov 25;250(22):8848-55.

111. Esteban JA, Salas M, Blanco L. Activation of S1 nuclease at neutral pH. Nucleic Acids Res. 1992;20(18):4932.

112. Flashner MS, Vournakis JN. Specific hydrolysis of rabbit globin messenger RNA by S1 nuclease. Nucleic Acids Res. 1977 Jul;4(7):2307-19.

113. Sutherland BM, Bennett PV, Sidorkina O, Laval J. Clustered DNA damages induced in isolated DNA and in human cells by low doses of ionizing radiation. Proc Natl Acad Sci U S A. 2000 Jan 4;97(1):103-8.

114. McNally L, Shaler RC, Baird M, Balazs I, DeForest P, Kobilinsky L. Evaluation of deoxyribonucleic acid (DNA) isolated from human bloodstains exposed to ultraviolet light, heat, humidity, and soil contamination. J Forensic Sci. 1989;34(5):1059-69.

115. Antheunisse J. Decomposition of nucleic acids and some of their degradation products by microorganisms. Antonie Van Leeuwenhoek. 1972;38(1):311-27.

116. O'Donovan P, Perrett CM, Zhang X, Montaner B, Xu YZ, Harwood CA, et al. Azathioprine and UVA light generate mutagenic oxidative DNA damage. Science. 2005 Sep 16;309(5742):1871-4.

117. Cadet J, Douki T. Oxidatively generated damage to DNA by UVA radiation in cells and human skin. J Invest Dermatol. 2011;131(5):1005-7.

118. Nicklas JA, Buel E. Quantification of DNA in forensic samples. Analytical and bioanalytical chemistry. 2003;376(8):1160-7.

119. Eckert WG, James SH. Interpretation of bloodstain evidence at crime scenes. CRC press; 1998.

120. Paabo S, Irwin DM, Wilson AC. DNA damage promotes jumping between templates during enzymatic amplification. J Biol Chem. 1990 Mar 15;265(8):4718-21.

121. Ballantyne J, National Ctr for Forensic Science, United States of America. Assessment and in vitro repair of damaged DNA templates. University of Central Florida, National Center for Forensic Science; 2006.

122. Marrone A, Ballantyne J. Changes in dry state hemoglobin over time do not increase the potential for oxidative DNA damage in dried blood. PloS one. 2009;4(4):e5110.